SOI: 1.1/TAS DOI: 10.15863/TAS

International Scientific Journal
Theoretical & Applied Science

p-ISSN: 2308-4944 (print) **e-ISSN:** 2409-0085 (online)

Year: 2018 **Issue:** 12 **Volume:** 68

Published: 21.12.2018 http://T-Science.org

QR – Issue QR – Article

SECTION 7. Mechanics and machine construction.

Denis Chemezov
M.Sc.Eng., Corresponding Member of International Academy of Theoretical and Applied Sciences, Lecturer of Vladimir Industrial College, Russian Federation
https://orcid.org/0000-0002-2747-552X
chemezov-da@yandex.ru

Alexandra Strunina
Lecturer of Vladimir Industrial College, Russian Federation

Irina Medvedeva
Master of Industrial Training,
Vladimir Industrial College, Russian Federation

Irina Pavluhina
Lecturer of Vladimir Industrial College, Russian Federation

Alexandr Korobkov
Student of Vladimir Industrial College, Russian Federation

Evgeny Varavin
Student of Vladimir Industrial College, Russian Federation

Tatyana Lukyanova
Lecturer of Vladimir Industrial College, Russian Federation

COMPARATIVE ANALYSIS OF AN IMPELLER GEOMETRY AT DIFFERENT HEADS OF A PUMP

***Abstract**: Impellers designing with ten blades at different heads of a hydraulic pump (from 5 to 25 m) by means of the Ansys Workbench software environment was carried out in the article. Three-dimensional models are presented and elements description of the radial impeller of the pump is given. Calculations of the impellers geometry were carried out at volume fluid flow rate (water) of 300 m^3/h. Profiles and geometric dimensions of the impeller blades are obtained in the spans: 0 and 1. It is determined that the radial impellers are recommended to be used at the pump head of 20 – 25 m. The most stable characteristic of the pump operation is observed in this range of heads. Tangential, meridional and relative velocities of fluid flow at the impeller blades are calculated.*

***Key words**: a radial impeller, a blade, a pump head, theta, beta, thickness, a shroud, a hub, fluid, a pump.*
***Language**: English*
***Citation**: Chemezov, D., et al. (2018). Comparative analysis of an impeller geometry at different heads of a pump. *ISJ Theoretical & Applied Science, 12 (68),* 149-192.
***Soi**: http://s-o-i.org/1.1/TAS-12-68-27 ***Doi**: crossref https://dx.doi.org/10.15863/TAS.2018.12.68.27

Introduction

Energy conversion of rotation of a motor shaft into fluid flow energy is performed by means of a radial impeller. Fluid moves from a center to a periphery of a device, i.e. centrifugal force occurs at rotation of the impeller. Vacuum is created in a central part of the radial impeller, which provides fluid supply under pressure to a suction pipe of the pump. The impellers are made of cast iron or steel.

Main elements of the radial impeller [1 – 10] are presented by the wire three-dimensional models in the Fig. 1 – 13. In a shroud it is located a hub with blades (the impeller). A gap is provided between maximum outer diameters of the shroud and the impeller, which is an outlet for moving fluid. Fluid is pumped into an inlet. The minimum and maximum diameters of the inlet equal to the minimum diameter of the hub and the minimum inner diameter of the pump shroud. The impeller blade profile is presented by end surfaces of the blades at the hub and the shroud. A periodic boundary defines a contour of a calculated cavity, which is located between the hub and the shroud. A centroid divides a passage area of the impeller in half. Mean lines characterize a number of the meridional flow surfaces. The camber surface of the blade is characterized by a maximum ordinate of the mean line of the profile. This parameter depends on the inlet angle and the outlet angle of fluid. The inlet and outlet edges of the blade are rounded, and a value of a rounding radius should be selected taking into account the requirements of hydrodynamics. The throat surface is defined as a distance between the low *theta* side and the high *theta* side along the blade surface. The radial impeller is built in the ***BladeGen*** module of the ***Ansys Workbench*** software environment.

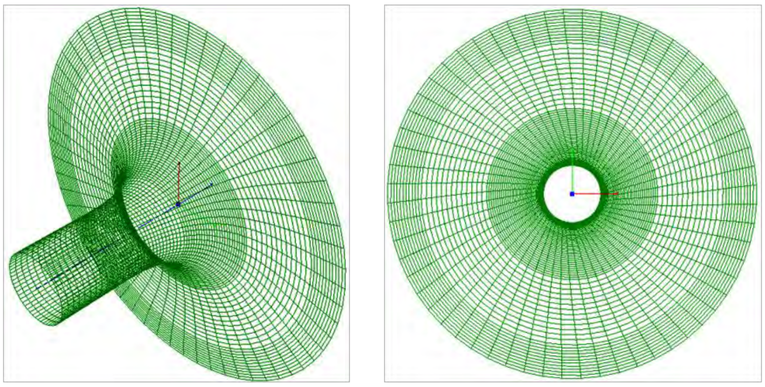

Figure 1 – The hub of the radial impeller.

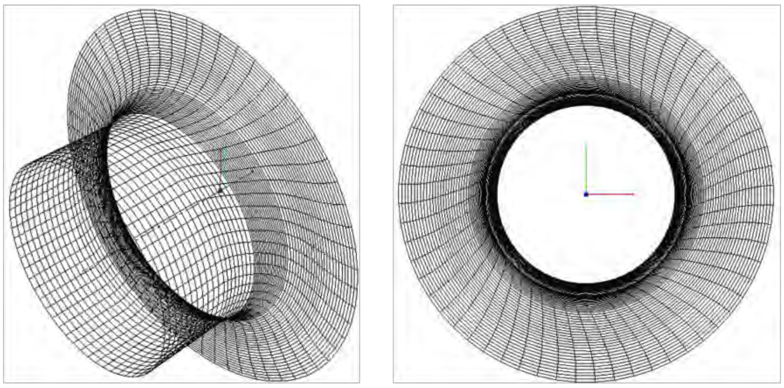

Figure 2 – The shroud of the radial impeller.

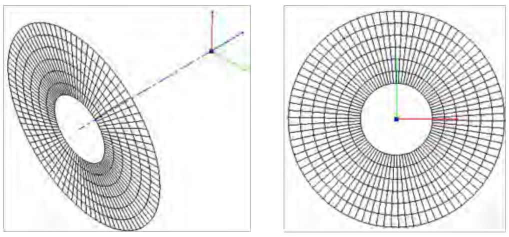

Figure 3 – The inlet of the radial impeller.

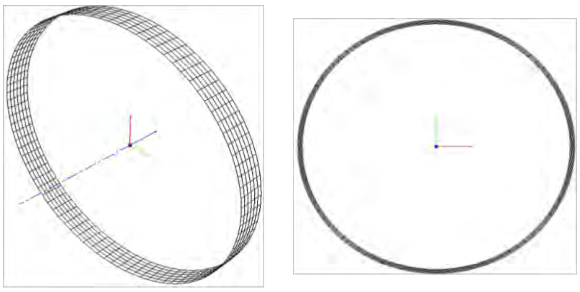

Figure 4 – The outlet of the radial impeller.

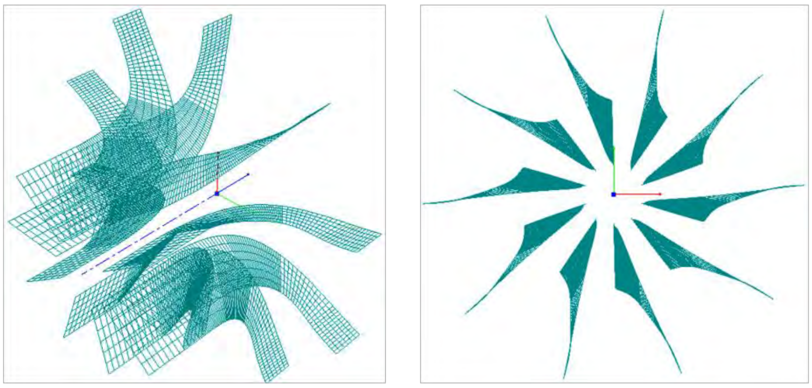

Figure 5 – The periodic of the radial impeller.

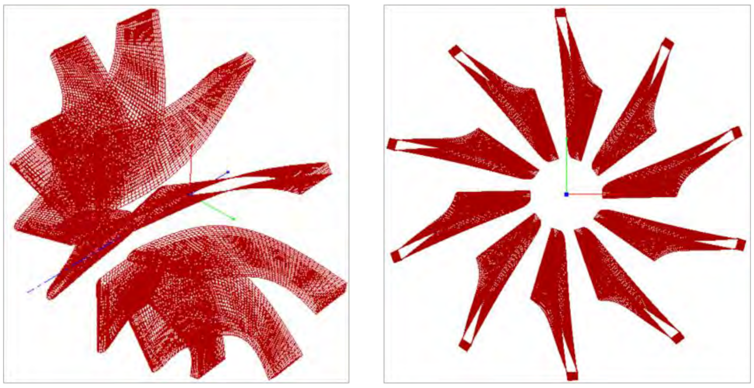

Figure 6 – The blades of the radial impeller.

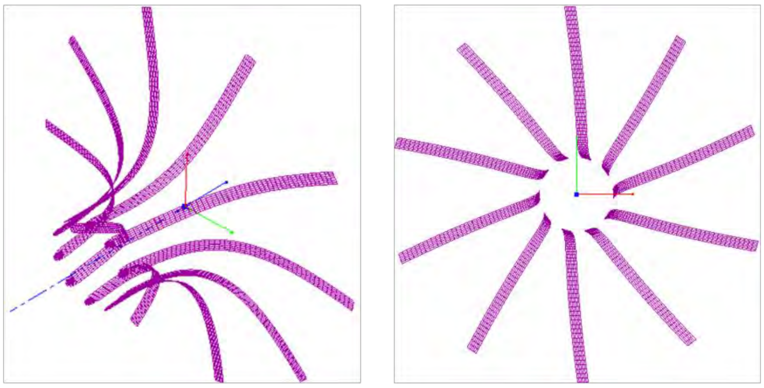

Figure 7 – The blades hub end of the radial impeller.

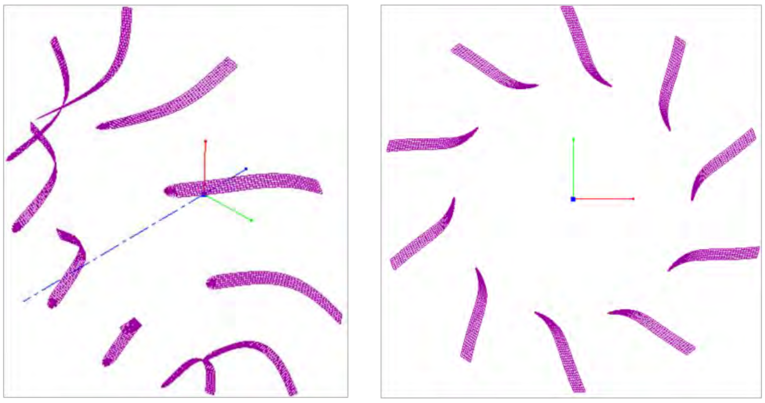

Figure 8 – The blades shroud end of the radial impeller.

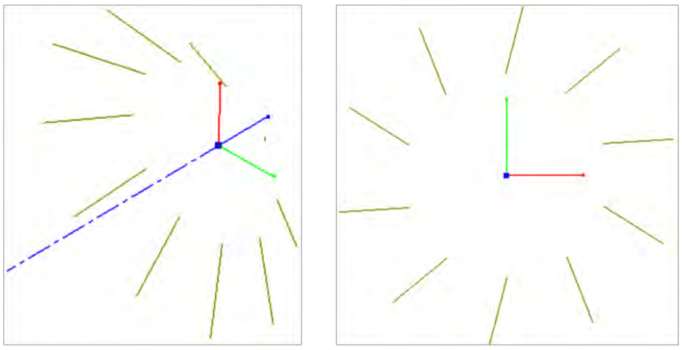

Figure 9 – The blades centroid of the radial impeller.

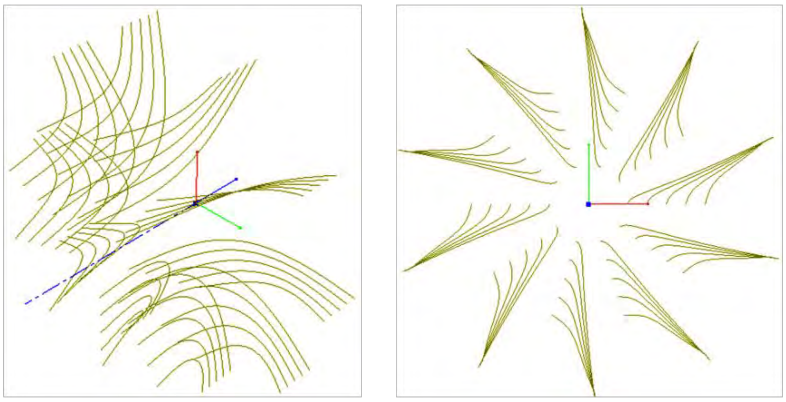

Figure 10 – The mean lines of the radial impeller.

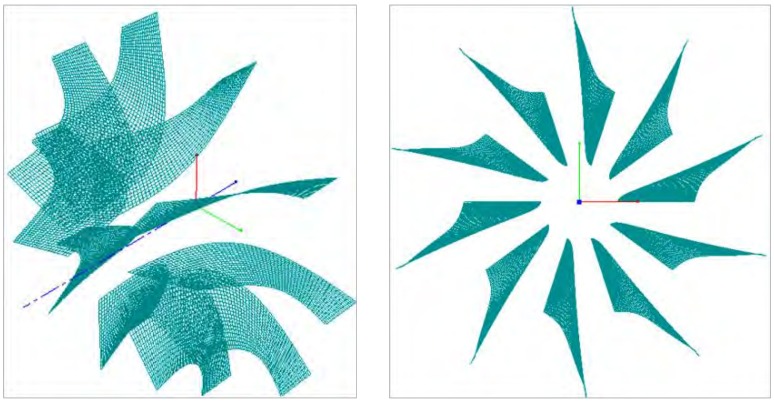

Figure 11 – The camber surfaces of the radial impeller.

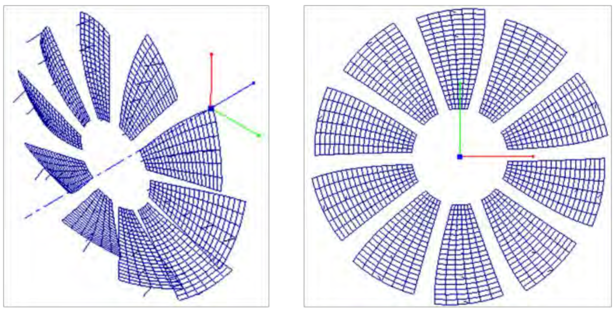

Figure 12 – The throat surfaces of the radial impeller.

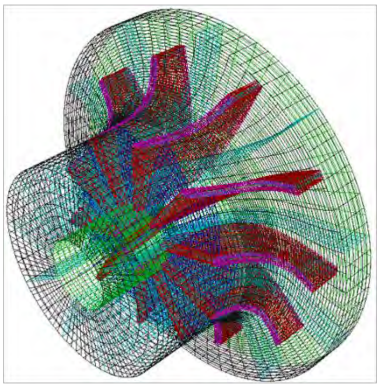

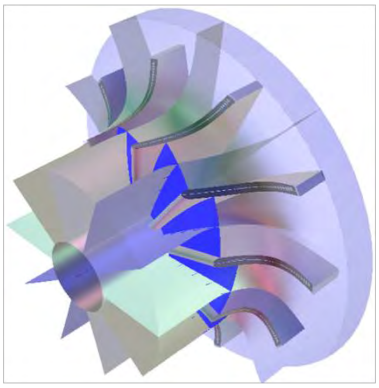

Figure 13 – The 3D model of the radial impeller.

The geometry calculation of the pump impellers

Initial operating conditions of the pump and the data for the geometry calculation of the impellers are presented in the table 1.

The geometry calculation of the impellers was carried out of 5 times at the different values of the pump head (*H*). The pump head is the sum of static and velocity heads.

Table 1. Operating conditions of the pump and the geometry of the radial impeller.

Operating conditions	
Duty	
Rotational speed	1500 rpm
Volume flow rate	300 m^3/hr
Density	1000 kg/m^3
Pump head	5/10/15/20/25 m
Inlet flow angle	90 deg
Merid. velocity ratio	1.1
Efficiencies	
Hydraulic	0.874
Volumetric	0.97
Mechanical	0.948
Pump	0.804
Geometry	
Hub diameter	
Shaft min. diam. factor	1.1
Dhub/Dshaft	1.5
Tip diameter	
Head coefficient	0.46
Tip diameter	280 mm
Leading edge blade angles	
Hub blade angle	27 deg
Mean blade angle	19 deg
Trailing edge blade angles	
Blade angle	22.5 deg
Rake angle	0 deg
Shroud	
Incidence	0 deg
Shroud blade angle	16 deg
Miscellaneous	
Number of blades	10
Thickness/tip diam.	0.03
Hub inlet draft angle	30 deg

The pump head varied in the range of 5 – 25 m. The remaining geometric and operating parameters of the radial impeller were constant. Volume flow rate of fluid by the value of 300 m^3/h was required at rotation speed of the radial impeller of 1500 rpm. Water with density of 1000 kg/m^3 was adopted as working fluid. The inlet flow angle is the angle at the leading edge of the impeller. The value of the inlet flow angle of fluid was taken 90 degrees for performing of the calculations. Approach flow without pre-rotation occurs at the given value of the inlet flow angle. The meridional velocity ratio is pattern of the linear velocity profile from the hub to the shroud at the leading edge of the radial impeller. Meridional velocity is less at the hub of the radial impeller at the value of the meridional velocity ratio of 1.1.

The efficiency coefficient of the pump is defined as the coefficients product of hydraulic, volumetric, and mechanical efficiencies. The coefficients values characterize losses of useful work of the pump at friction of the mating elements of the device.

The shaft minimum diameter factor is the safety factor of the pump shaft in conditions of maximum allowable shear stress of material. The one tenth of the factor (1.1) is increasing of the shaft diameter by 10%. The ratio of the impeller hub diameter to the shaft diameter (*Dhub/Dshaft*) was taken 1.5. The tip diameter was set to 280 mm at the adopted pump head coefficient equal to 0.46. The leading edge blade angles are characterized by the hub blade angle (27 degrees) and the mean blade angle (19 degrees). The trailing edge blade angles are characterized by the blade angle (22.5 degrees) and the rake angle (0 degrees). The blade angle at the shroud by the value of 16 degrees was adopted at designing of the impeller. The incidence angle at the shroud was selected by default 0 degrees.

The adopted number of the impellers blades is 10 pieces. This number of the blades gives greater control over flow direction in the pump impeller. The ratio of thickness to the tip diameter is used for determining of the impeller blade thickness. The ratio of thickness to the tip diameter equal to 0.03 indicates about a low probability of blockage to fluid flow. The hub inlet draft angle (30 degrees) is the angle between the hub and the horizontal line at the hub inlet. The hub radius of the pump impeller depends on the value of this angle.

The calculated parameters of the impeller elements in the different sections (from stub to peripheral) are presented in the summary table 2.

Table 2. The layers parameters.

Parameters	Pump head, m				
	5	10	15	20	25
Span: 0					
1. Layer	**Value**				
B2B throat length 0	23.2998	30.7859	33.0261	35.0692	36.0579
Segment 0 (0 to 0)	23.2997	30.7559	32.9884	35.018	36.0186
Crv throat length 0	23.2997	30.7559	32.9884	35.018	36.0186
LE pitch	32.6379	34.94	38.1708	42.7978	46.9774
TE pitch (S)	64.7102	97.6394	121.378	138.501	152.753
Centroid:Z	-10.3934	-6.99712	-3.1923	-1.75024	-1.5597
Centroid:R	48.4668	67.2025	81.5823	92.5206	101.509
Centroid:T	-38.8	-38.3	-45.6	-54.0	-61.0
Centroid:Mp	0.589379	0.805987	0.877109	0.864041	0.849385
Centroid:M	23.0234	38.4933	48.5125	54.0931	58.5061
Airfoil area	327.405	582.996	893.181	1224.9	1574.36
2. Blade & layer	**Value**				
3D meanline length	67.8987	99.3529	130.444	158.032	183.85
Camber length	67.9001	99.3554	130.448	158.038	183.859
Cord length (C)	67.1055	96.7405	127.599	155.85	182.175
Meridional length (M)	39.9246	65.4698	83.0066	93.8869	102.905
Stagger angle	-53.5	-47.4	-49.4	-53.0	-55.6
Solidity (C/S)	1.03702	0.990793	1.05126	1.12526	1.19261
Pitch cord ratio (S/C)	0.964305	1.00929	0.951243	0.888686	0.838494
3. Bezier	**Value**				
Stagger angle	51.8	43.6	45.5	49.8	53.0
LE theta angle	0.1	0.2	0.2	0.2	0.2
LE beta angle	41.5	31.4	33.5	39.6	44.1
TE beta angle	67.7	68.1	67.9	67.7	67.6
LE wedge angle	-2.2	-2.2	-2.8	-3.1	-3.2

TE wedge angle	0.6	0.6	0.6	0.6	0.6
LE thickness	4.9514	5.99524	6.96641	7.85943	8.66235
TE thickness	5.01253	6.07905	7.06994	7.98399	8.80553
4. Advanced side1 point	**Value**				
First point %M'	20.0	20.0	20.0	20.0	20.0
Last point %M'	80.0	80.0	80.0	80.0	80.0
Linear point %M'	30.0	30.0	30.0	30.0	30.0
5. Advanced side2 point	**Value**				
First point %M'	30.0	30.0	30.0	30.0	30.0
Last point %M'	80.0	80.0	80.0	80.0	80.0
Linear point %M'	0.0	0.0	0.0	0.0	0.0
Span: 0.2500					
1. Layer	**Value**				
B2B throat length 0	26.0818	38.4671	39.2628	38.2518	37.3117
Segment 0 (0 to 0)	26.0781	38.3506	39.1432	38.1645	37.2594
Crv throat length 0	26.0781	38.3506	39.1432	38.1645	37.2594
LE pitch	47.3035	48.9666	51.3608	54.8135	57.9361
TE pitch (S)	75.8122	101.529	122.008	138.501	152.753
Centroid:Z	-25.891	-25.6256	-20.0568	-16.1472	-13.9837
Centroid:R	59.7521	73.868	85.6612	95.5541	104.129
Centroid:T	-38.0	-37.9	-45.0	-53.2	-60.1
Centroid:Mp	0.420255	0.55918	0.633694	0.658856	0.676587
Centroid:M	21.8246	32.8187	41.1055	46.7755	51.7116
Airfoil area	373.976	572.247	861.731	1199.33	1559.14
2. Blade & layer	**Value**				
3D meanline length	77.6836	97.8091	126.18	155.099	182.455
Camber length	77.6849	97.8112	126.184	155.104	182.463
Cord length (C)	77.4054	96.77	125.068	154.259	181.797
Meridional length (M)	39.171	57.2882	72.3401	83.6417	93.5598
Stagger angle	-59.6	-53.7	-54.7	-57.2	-59.0
Solidity (C/S)	1.02102	0.953126	1.02508	1.11377	1.19014
Pitch cord ratio (S/C)	0.979417	1.04918	0.975534	0.89785	0.840238
Span: 0.5000					
1. Layer	**Value**				
B2B throat length 0	28.1162	36.7428	37.906	36.4677	35.5472
Segment 0 (0 to 0)	28.0973	36.6617	37.7949	36.3734	35.4738
Crv throat length 0	28.0973	36.6617	37.7949	36.3734	35.4738
LE pitch	61.9692	62.9933	64.5508	66.8292	68.8948
TE pitch (S)	86.9141	105.419	122.638	138.501	152.753
Centroid:Z	-41.6684	-44.5786	-37.1857	-30.729	-26.5341
Centroid:R	70.985	80.2918	89.5001	98.4238	106.642
Centroid:T	-37.2	-37.2	-44.1	-52.2	-58.9
Centroid:Mp	0.320383	0.39399	0.459632	0.504708	0.54221
Centroid:M	20.7071	27.2334	33.9249	39.7815	45.2645
Airfoil area	427.293	576.717	848.986	1191.14	1559.11
2. Blade & layer	**Value**				
3D meanline length	88.7124	98.91	124.694	154.393	182.775
Camber length	88.7137	98.9117	124.697	154.398	182.783
Cord length (C)	88.6499	98.6635	124.434	154.188	182.603
Meridional length (M)	38.881	49.716	62.3336	73.9907	84.7322
Stagger angle	-64.0	-59.7	-59.9	-61.3	-62.4
Solidity (C/S)	1.01997	0.935921	1.01464	1.11326	1.19541
Pitch cord ratio (S/C)	0.98042	1.06847	0.985568	0.898262	0.83653
Span: 0.7500					
1. Layer	**Value**				
B2B throat length 0	28.6997	32.6836	33.1581	32.5563	32.419
Segment 0 (0 to 0)	28.6716	32.5919	33.0416	32.4384	32.3101
Crv throat length 0	28.6716	32.5919	33.0416	32.4384	32.3101
LE pitch	76.6348	77.0199	77.7408	78.845	79.8535

TE pitch (S)	98.0161	109.308	123.268	138.501	152.753
Centroid:Z	-57.6932	-63.9253	-54.7011	-45.5738	-39.2533
Centroid:R	82.2844	86.8073	93.3748	101.29	109.141
Centroid:T	-36.3	-36.0	-42.8	-50.7	-57.6
Centroid:Mp	0.255572	0.279544	0.33318	0.388123	0.437373
Centroid:M	19.7555	22.1866	27.4634	33.4823	39.4281
Airfoil area	486.85	597.648	856.517	1201.45	1575.2
2. Blade & layer	**Value**				
3D meanline length	100.576	102.451	125.841	155.728	184.642
Camber length	100.578	102.453	125.843	155.732	184.649
Cord length (C)	100.554	102.418	125.807	155.697	184.619
Meridional length (M)	39.0661	43.0816	53.3736	65.2198	76.6254
Stagger angle	-67.1	-65.1	-64.9	-65.2	-65.5
Solidity (C/S)	1.02589	0.936967	1.0206	1.12415	1.20861
Pitch cord ratio (S/C)	0.974762	1.06727	0.979817	0.889558	0.827395
Span: 1.000					
1. Layer	**Value**				
B2B throat length 0	29.1029	28.7079	28.172	28.197	28.7868
Segment 0 (0 to 0)	29.0676	28.6157	28.0639	28.081	28.674
Crv throat length 0	29.0676	28.6157	28.0639	28.081	28.674
LE pitch	91.3006	91.0465	90.9308	90.8607	90.8121
TE pitch (S)	109.118	113.198	123.898	138.501	152.753
Centroid:Z	-73.928	-83.7056	-72.748	-60.7837	-52.1925
Centroid:R	93.7295	93.7777	97.6091	104.321	111.722
Centroid:T	-35.4	-34.5	-40.9	-49.0	-55.9
Centroid:Mp	0.211152	0.202424	0.245067	0.302507	0.357096
Centroid:M	19.0061	18.1594	22.307	28.2962	34.4824
Airfoil area	551.495	635.345	885.252	1230.95	1607.84
2. Blade & layer	**Value**				
3D meanline length	113.026	108.032	129.286	158.847	187.866
Camber length	113.028	108.033	129.289	158.851	187.873
Cord length (C)	112.936	107.938	129.203	158.787	187.834
Meridional length (M)	39.7187	37.8792	46.07	57.7218	69.4783
Stagger angle	-69.4	-69.5	-69.1	-68.7	-68.3
Solidity (C/S)	1.03499	0.953535	1.04282	1.14646	1.22966
Pitch cord ratio (S/C)	0.966192	1.04873	0.958942	0.872247	0.813231
3. Bezier	**Value**				
Stagger angle	69.5	69.6	69.3	68.9	68.5
LE theta angle	0.0	0.0	0.0	0.0	0.0
LE beta angle	73.9	74.1	73.3	72.1	70.9
TE beta angle	66.7	66.7	66.8	67.0	67.1
LE wedge angle	-0.1	-0.1	-0.1	-0.2	-0.3
TE wedge angle	0.3	0.5	0.6	0.6	0.6
LE thickness	4.97315	6.03083	7.01342	7.91714	8.72736
TE thickness	4.99269	6.06864	7.06667	7.98304	8.80505
4. Advanced side1 point	**Value**				
First point %M'	20.0	20.0	20.0	20.0	20.0
Last point %M'	80.0	80.0	80.0	80.0	80.0
Linear point %M'	30.0	30.0	30.0	30.0	30.0
5. Advanced side2 point	**Value**				
First point %M'	30.0	30.0	30.0	30.0	30.0
Last point %M'	80.0	80.0	80.0	80.0	80.0
Linear point %M'	0.0	0.0	0.0	0.0	0.0

Main integral characteristics of the cross sections of the profiled pump impellers blades are given in the table. *Span 0.000* is the stub section of the impeller blade; *span 1.000* is the peripheral section of the impeller blade. The calculation of a pitch at the leading edge of the blade (*LE pitch*), the pitch at the trailing edge of the blade (*TE pitch*), the airfoil area, a cord length (*C*), the meridional length (*M*), the stagger angle, solidity (*C/S*), the pitch cord ratio (*S/C*) and the other parameters was performed.

At considering of the blades characteristics in the stub and peripheral sections, it could be argued that:

1. The pitch at the leading edge of the impeller blade in the stub section increases with increasing of the pump head, and the pitch in the peripheral section decreases.

2. The pitches at the trailing edge of the impeller blade are the same in the stub and peripheral sections at the pump heads of 20 and 25 m.

3. Decreasing of the airfoil area of the impeller blade is almost twice observed at the pump head of 5 m.

The contours and the dependencies graphs of the main elements geometry of the impellers from the pump head are presented in the Fig. 14 – 45. The flowing parts of the impellers blades and fluid flow direction are displayed in the meridional configuration. The blade channels (two adjacent impeller blades) are shown in the Fig. 15. *Theta* is circumferential coordinate of the mean line points in a cylindrical coordinate system, an axis of which coincides with the axis of an engine. *Beta* (axial) is the angle between a tangent to the mean line of the profile and the axis of the impeller. *Theta* changes in the range of 0...-100 degrees. The maximum negative value of the angle is reached at the trailing edge of the blade at the pump head of 25 m. *Beta* changes in the range of 120…165 degrees. The value of the angle decreases in the stub section of the impeller blade. Thickness changing of the impellers blades is in the range of 0.09 to 0.5 mm. Changing of the inverse radius of curvature of the blade at the hub and the shroud of the impeller in meridional fraction from the leading edge to the trailing edge are shown in the Fig. 19. Maximum increasing of the inverse radius of curvature of the blade is observed at the trailing edge. The dependencies of the inverse radius of curvature of the blade in meridional fraction from the leading edge to the trailing edge (the parameters *mean*, *side1* and *side2*) are presented in the Fig. 20. *Mean* is a default option and specifies that the *theta* values are for location of the mean line. *Side1* specifies that the *theta* values locate the side of the blade (at the larger *theta* value). *Side2* specifies that the *theta* values locate the side of the blade (at the smaller *theta* value). The inverse radius of curvature of the impeller blade (the leading edge) at *mean* and *side1* has the positive values. The values changing of *theta* and *beta* at the leading and trailing edges of the impellers blades in the range of the stub/peripheral sections are defined in the Fig. 21 and 22. *Theta* at the leading edge of the blade is 0 degrees; *theta* at the trailing edge is 65...92 degrees. In the stub section *Beta* at the leading edge of the blade is more than at the trailing edge, and in the peripheral section is vice versa. A height distribution of the minor and major radii of ellipses of the leading edge of the impeller blade is shown in the Fig. 23. The relative height of the impeller blade is plotted along the horizontal axis, the values of the edges radii in mm are plotted along the vertical axis. Changing of the lean angle of the impeller blade at the hub and the shroud from the relative axial chord is calculated in the Fig. 24. Significant changing of the values of this angle is determined at the pump head of 20 – 25 m. The quasi-orthogonal area was calculated with and without the flow angle correction of fluid, with and without the blades. It is determined that the quasi-orthogonal area of the blade with correction in 2 – 3 times is less than the quasi-orthogonal area of the blade without correction. The airfoil areas of the impellers blades in the height are calculated on the graphs (the Fig. 26). The airfoil area of the blade from the hub to the shroud increases linearly at the pump head of 5 m. The airfoil area decreases according to a non-linear law at the pump head of 15 – 20 m at the distance from the stub section to the mean line, and the airfoil area increases according to the non-linear law at the distance from the mean line to the peripheral section. The maximum spherical diameter at the leading edge of the impeller blade is 85 mm at the pump head of 10 m. This is the maximum value of this parameter. The dependencies of *theta* and *beta* from *M-Prime* (the current blade angle with the horizontal axis using the radius normalized meridional distance), *M* (the current blade angle with the horizontal axis using the meridional distance), *Z* (the current blade angle with the horizontal axis using axial location) and *R* (the current blade angle with the horizontal axis using radial location) are shown in the Fig. 28 – 31. Changing of *theta* and *beta* from the stub to peripheral sections of the impellers blades are presented in the Fig. 32 – 39. *Theta* from *M* at the leading edge of the blade (in all sections) is 0 degrees; *theta* from *M* at the trailing edge is 65 degrees. The impeller blade profile has maximum curvature at the high pump heads. The dependencies of *beta* from *theta* for all sections are presented in the Fig. 40. It is noted that in the stub section *beta* decreases, and in the peripheral section *beta* increases.

A

B

C

D

E

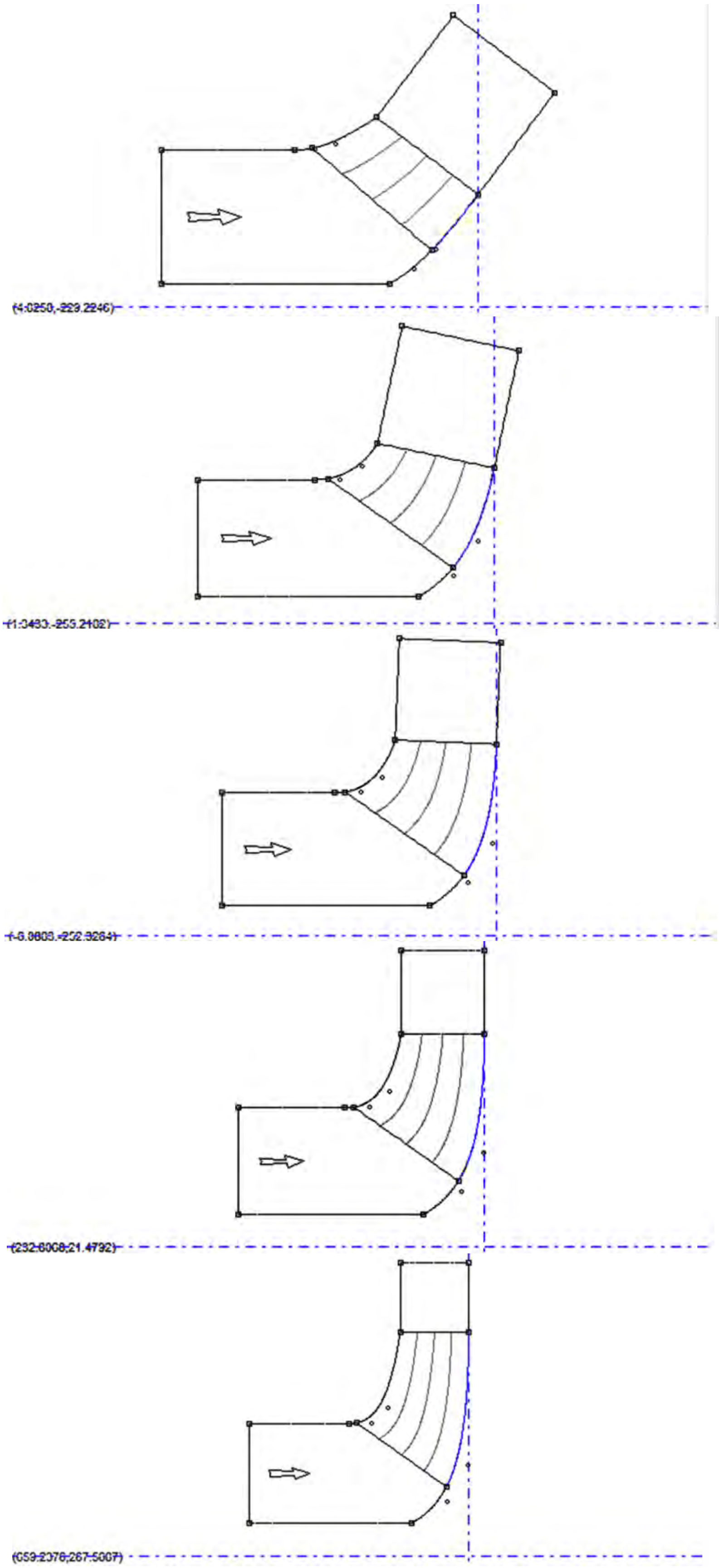

Figure 14 – The meridional configuration of the impeller blade: A) *H* = 5 m, B) *H* = 10 m, C) *H* = 15 m, D) *H* = 20 m, E) *H* = 25 m.

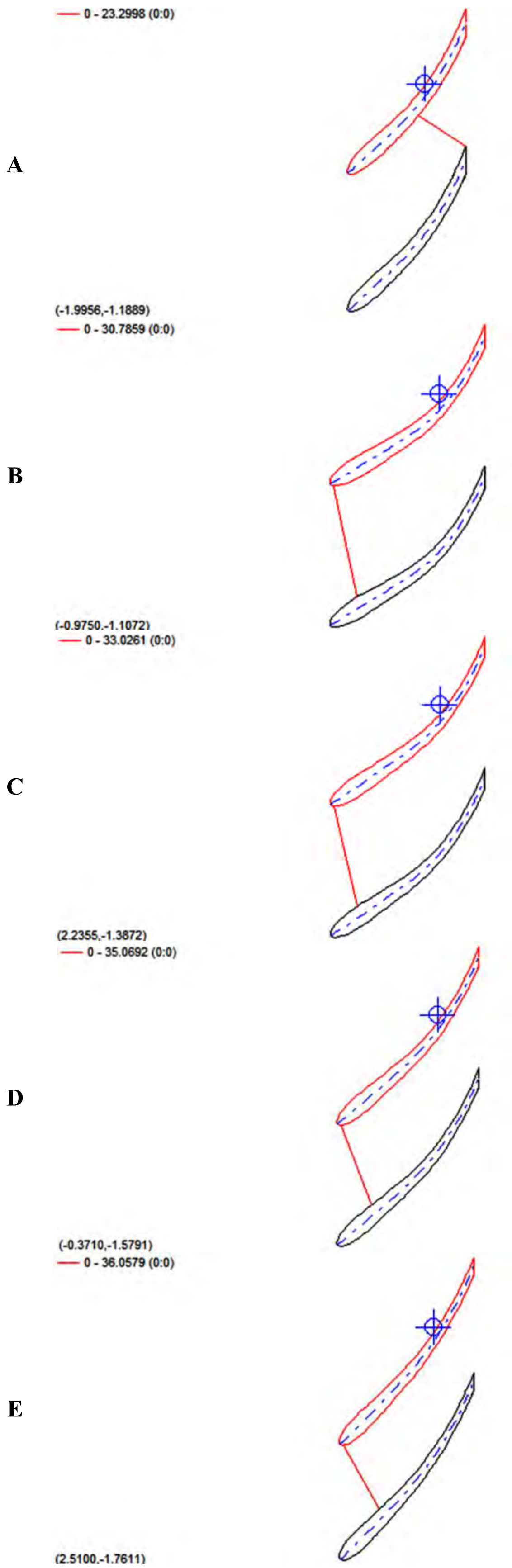

Figure 15 – The blade-to-blade view: A) H = 5 m, B) H = 10 m, C) H = 15 m, D) H = 20 m, E) H = 25 m.

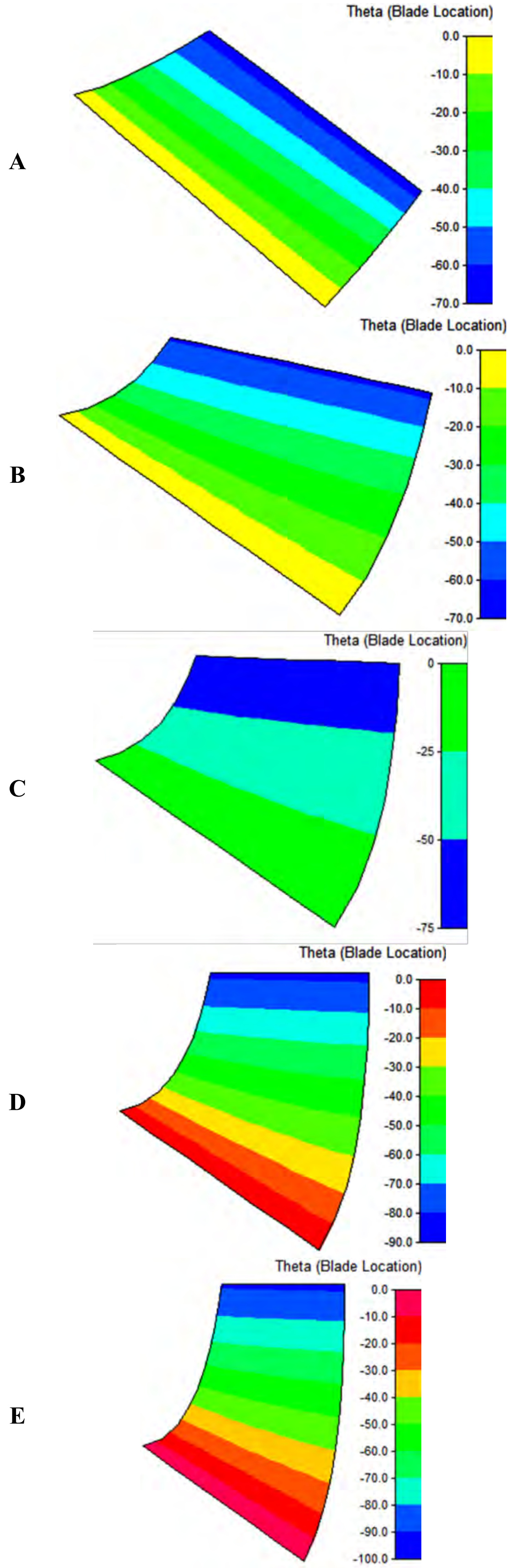

Figure 16 – Theta (blade location): A) *H* = 5 m, B) *H* = 10 m, C) *H* = 15 m, D) *H* = 20 m, E) *H* = 25 m.

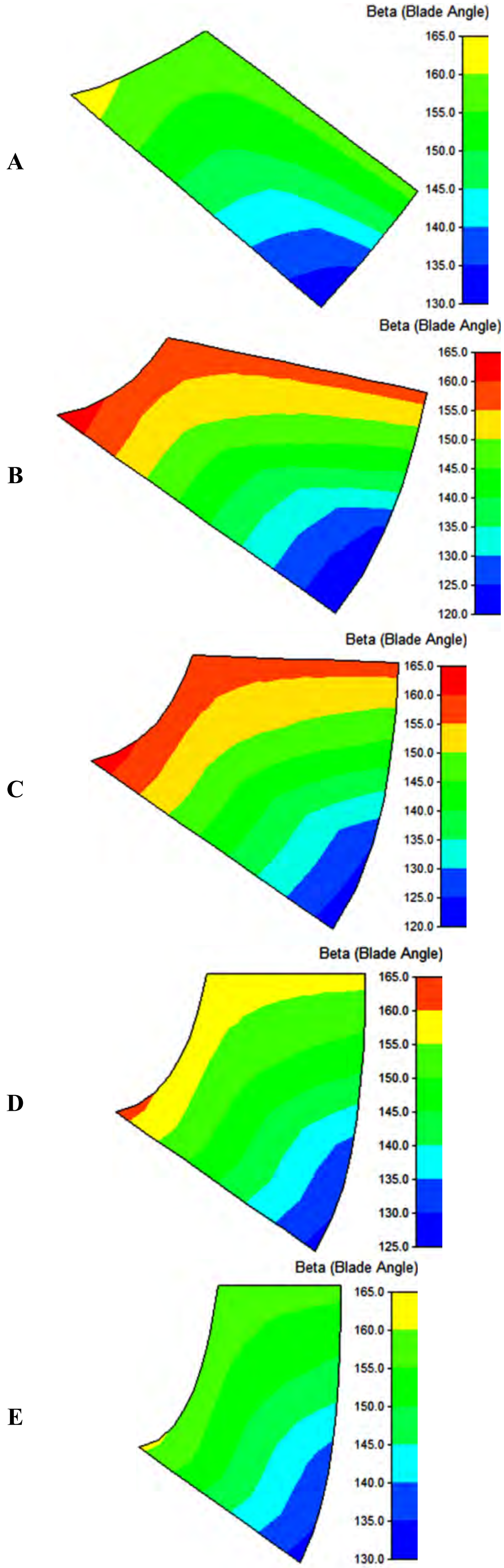

Figure 17 – Beta (blade angle): A) *H* = 5 m, B) *H* = 10 m, C) *H* = 15 m, D) *H* = 20 m, E) *H* = 25 m.

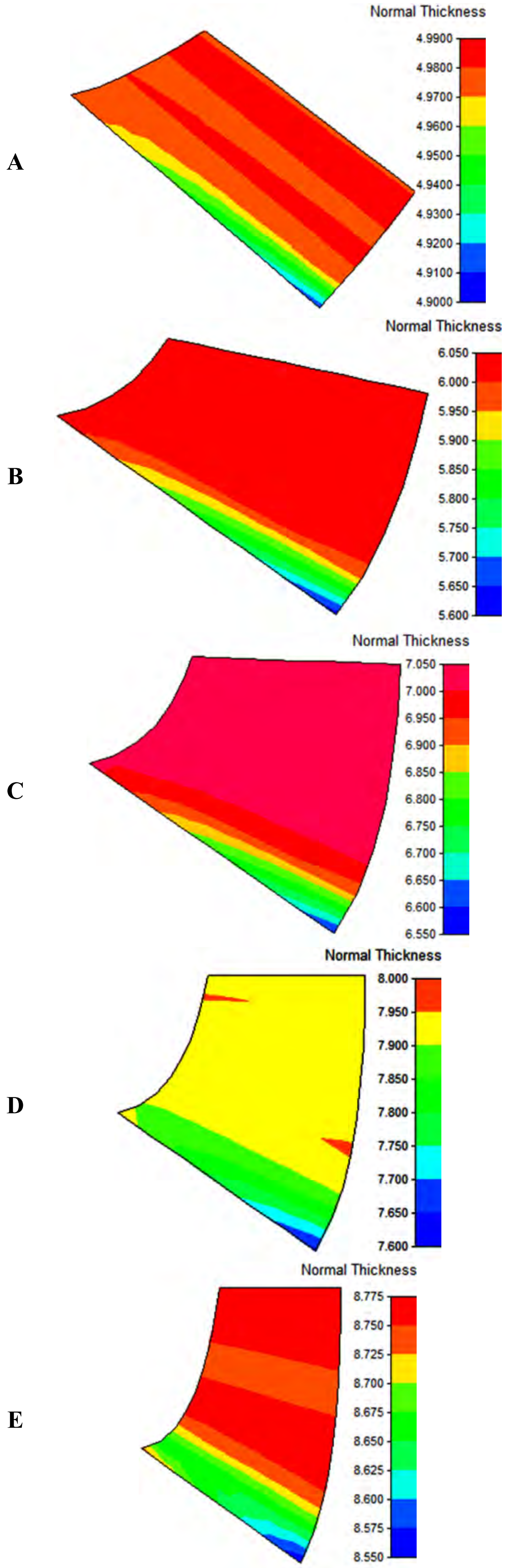

Figure 18 – Normal thickness: A) *H* = 5 m, B) *H* = 10 m, C) *H* = 15 m, D) *H* = 20 m, E) *H* = 25 m.

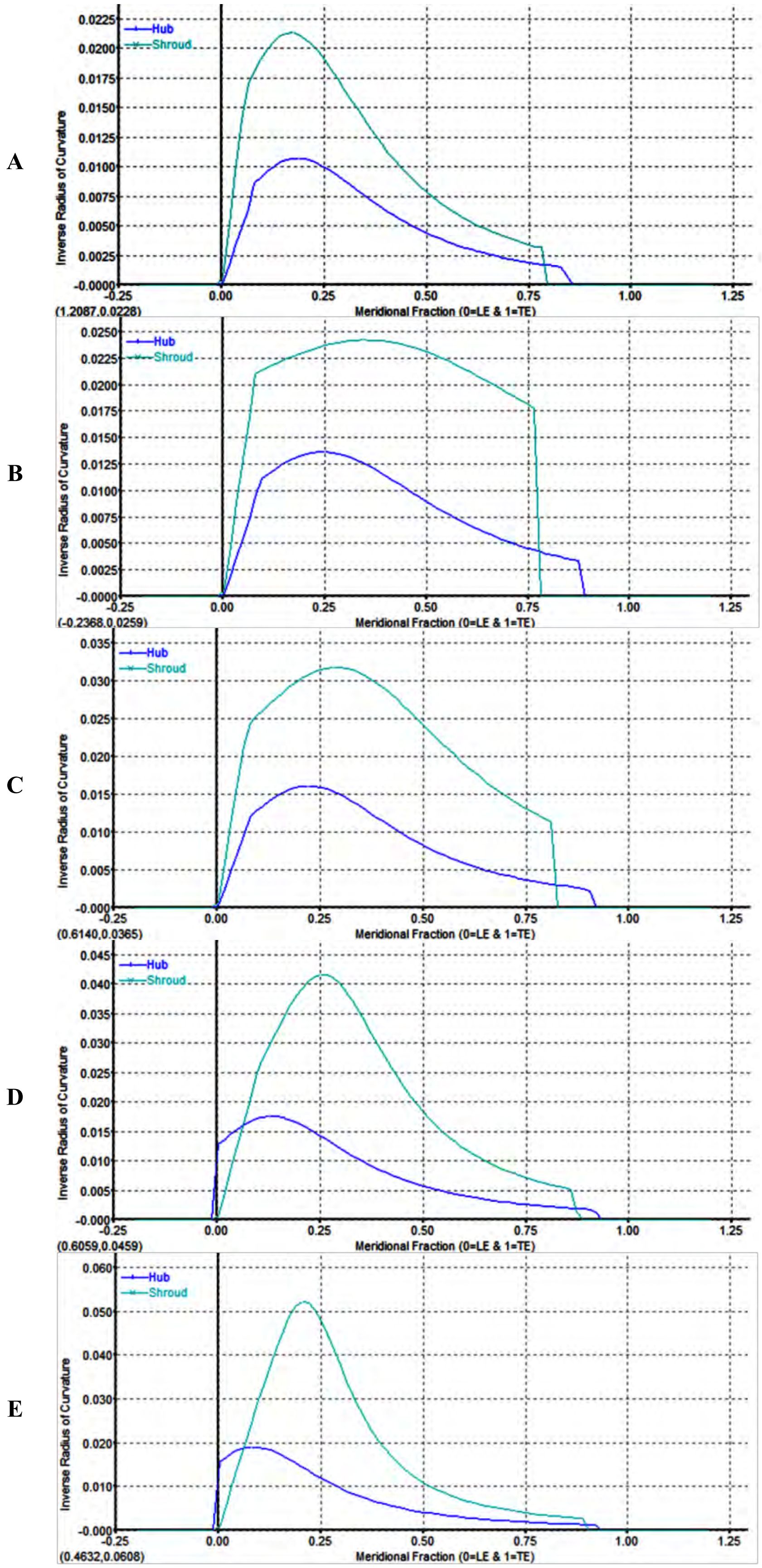

Figure 19 – The meridional curvature graph: A) $H = 5$ m, B) $H = 10$ m, C) $H = 15$ m, D) $H = 20$ m, E) $H = 25$ m.

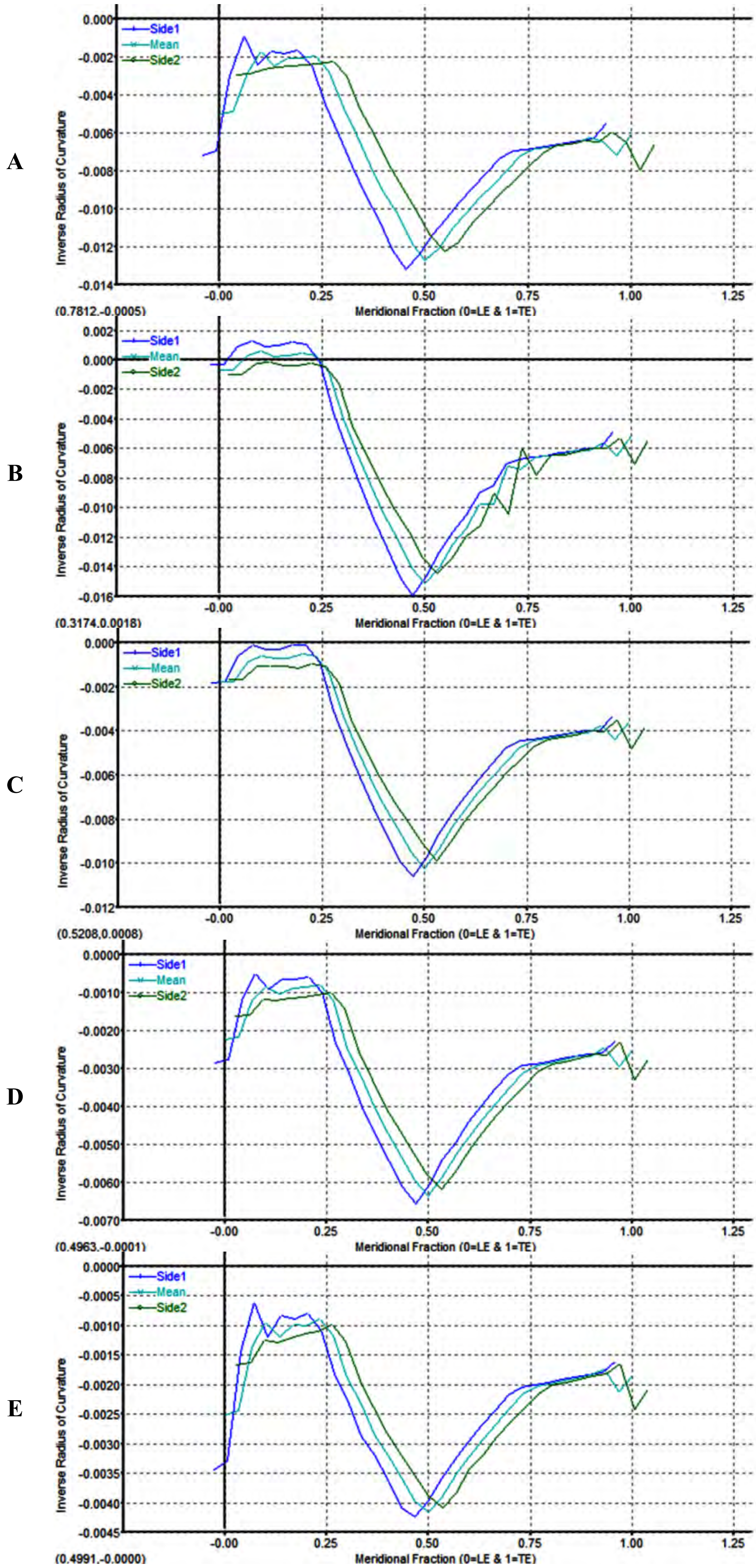

Figure 20 – The blade-to-blade curvature graph: A) *H* = 5 m, B) *H* = 10 m, C) *H* = 15 m, D) *H* = 20 m, E) *H* = 25 m.

A

B

C

D

E

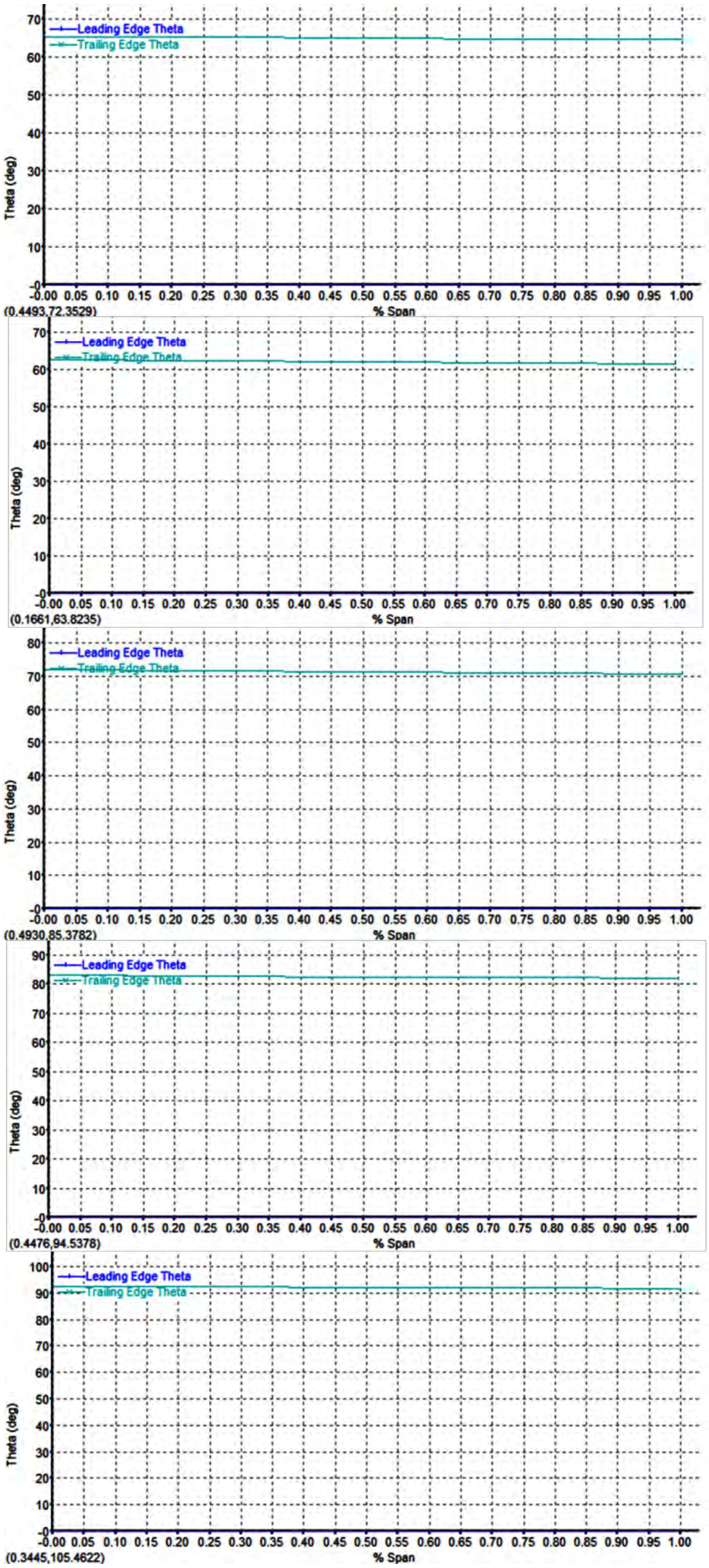

Figure 21 – The LE/TE theta graph: A) H = 5 m, B) H = 10 m, C) H = 15 m, D) H = 20 m, E) H = 25 m.

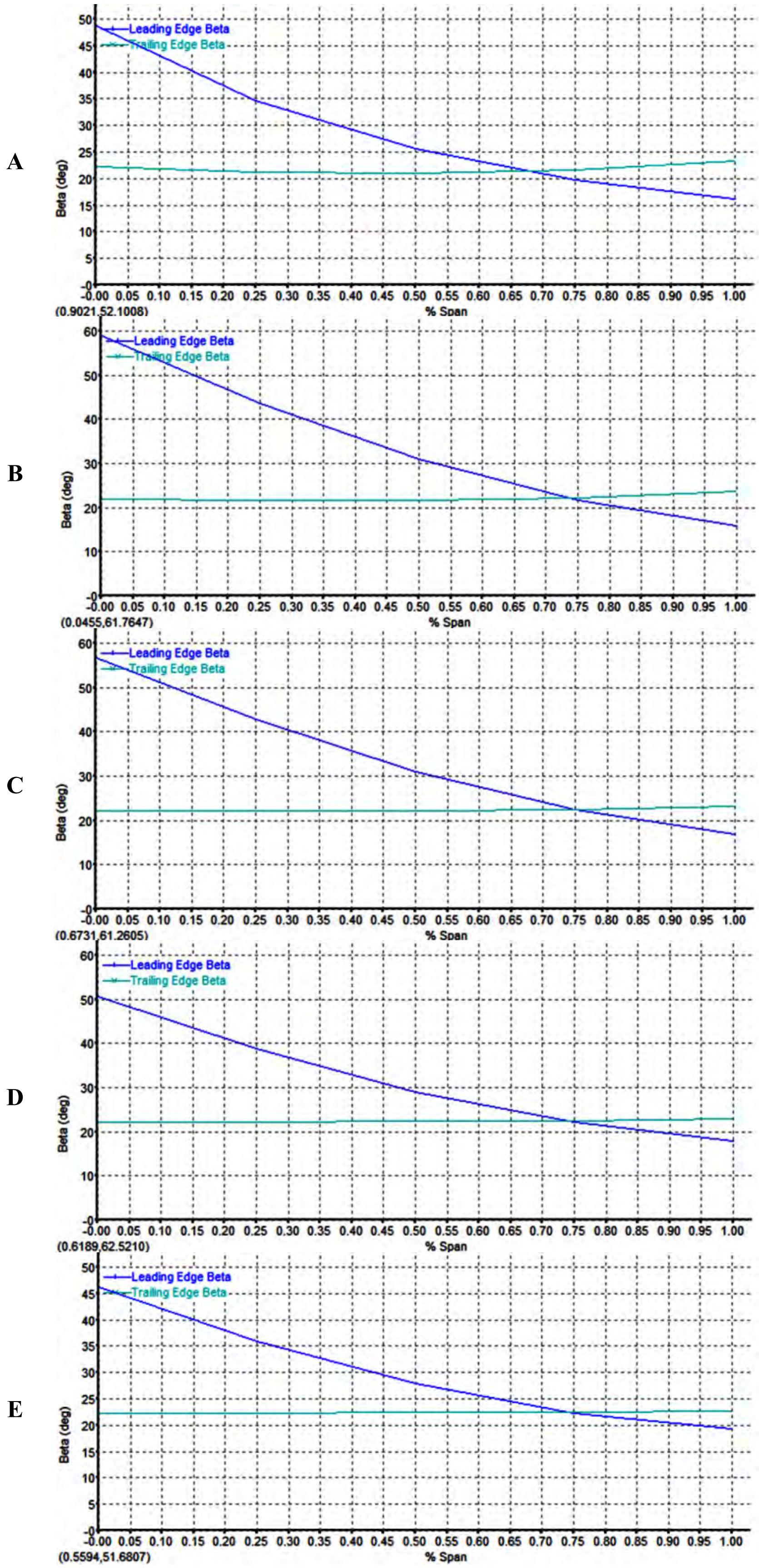

Figure 22 – The LE/TE beta graph: A) H = 5 m, B) H = 10 m, C) H = 15 m, D) H = 20 m, E) H = 25 m.

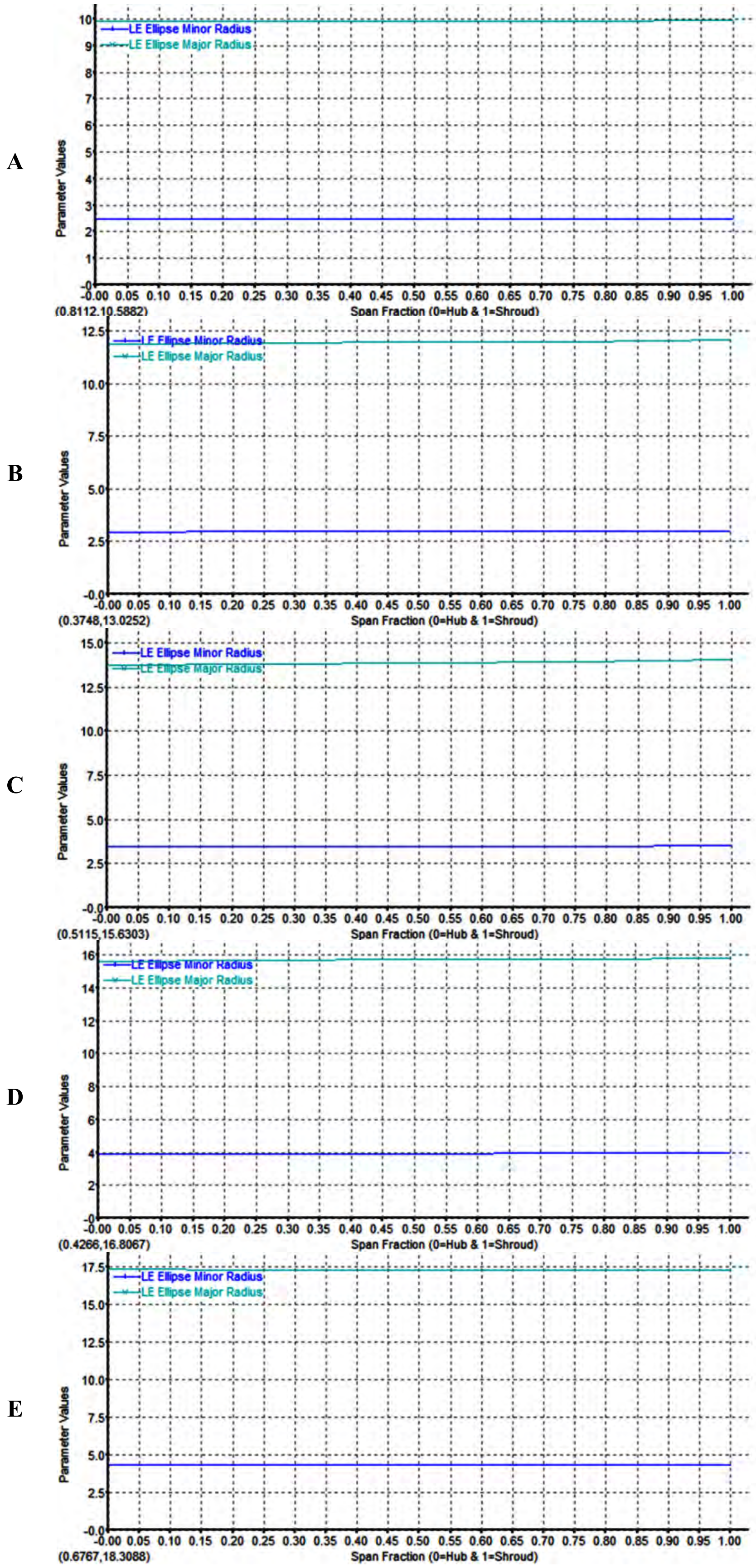

Figure 23 – The LE/TE parameter graph: A) $H = 5$ m, B) $H = 10$ m, C) $H = 15$ m, D) $H = 20$ m, E) $H = 25$ m.

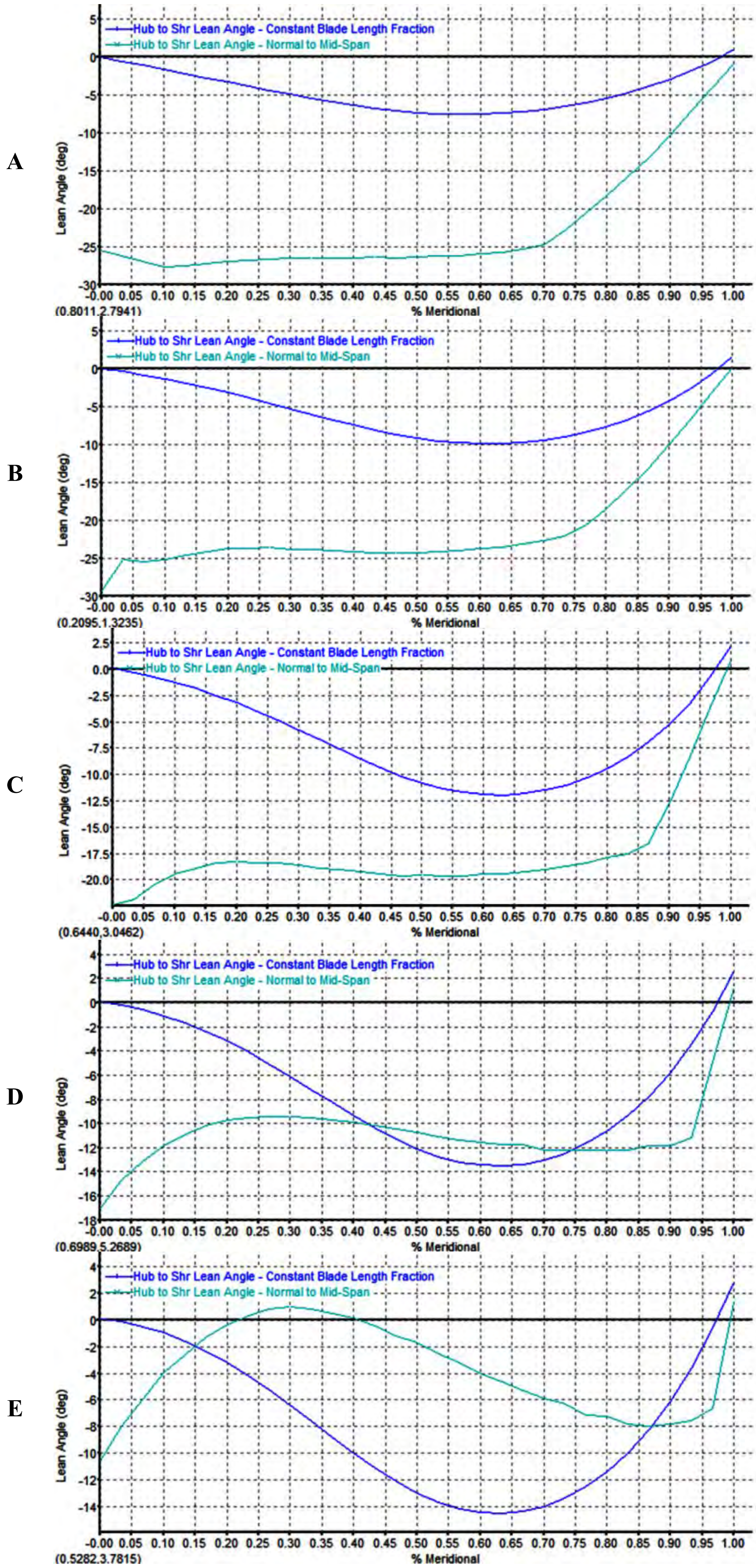

Figure 24 – The blade lean angle graph: A) *H* = 5 m, B) *H* = 10 m, C) *H* = 15 m, D) *H* = 20 m, E) *H* = 25 m.

A

B

C

D

E

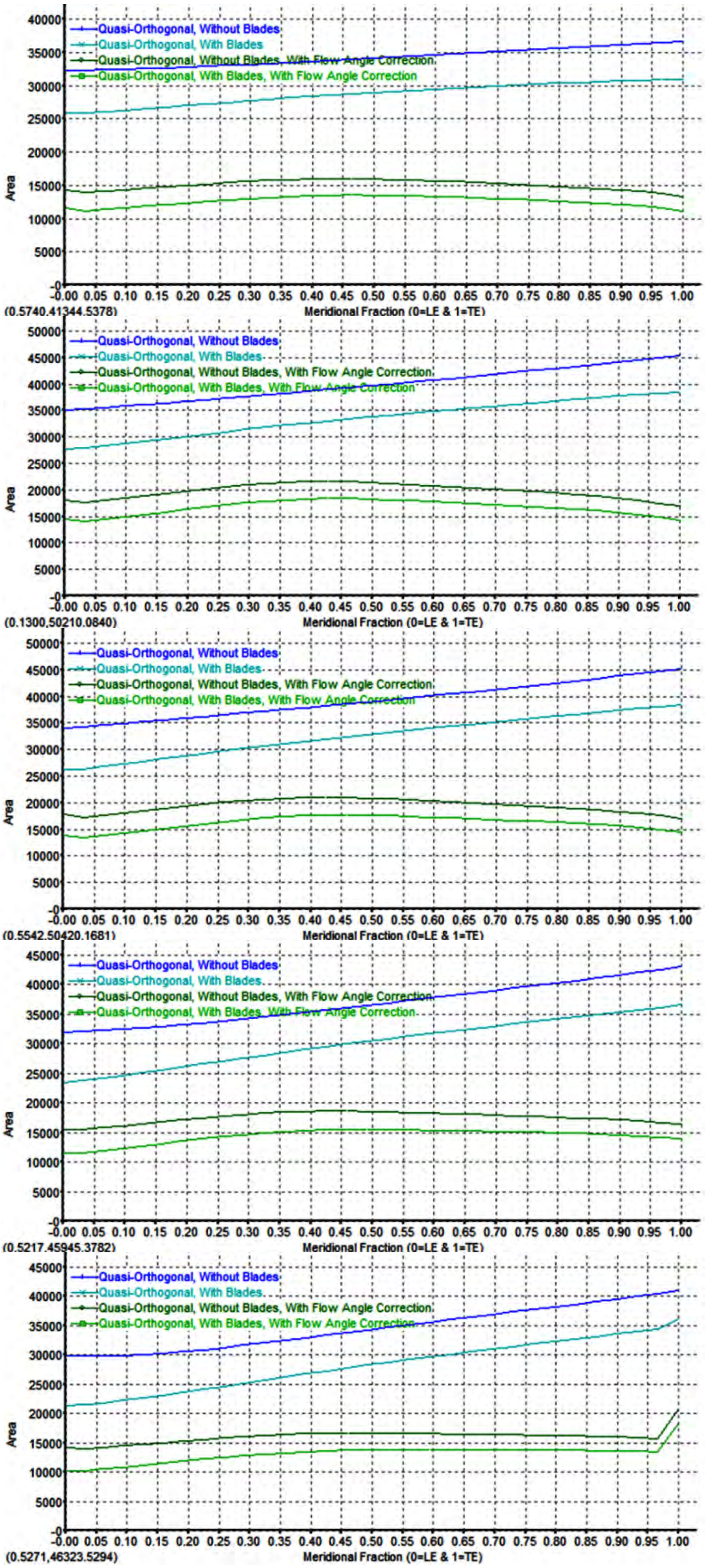

Figure 25 – The quasi-orthogonal area graph: A) *H* = 5 m, B) *H* = 10 m, C) *H* = 15 m, D) *H* = 20 m, E) *H* = 25 m.

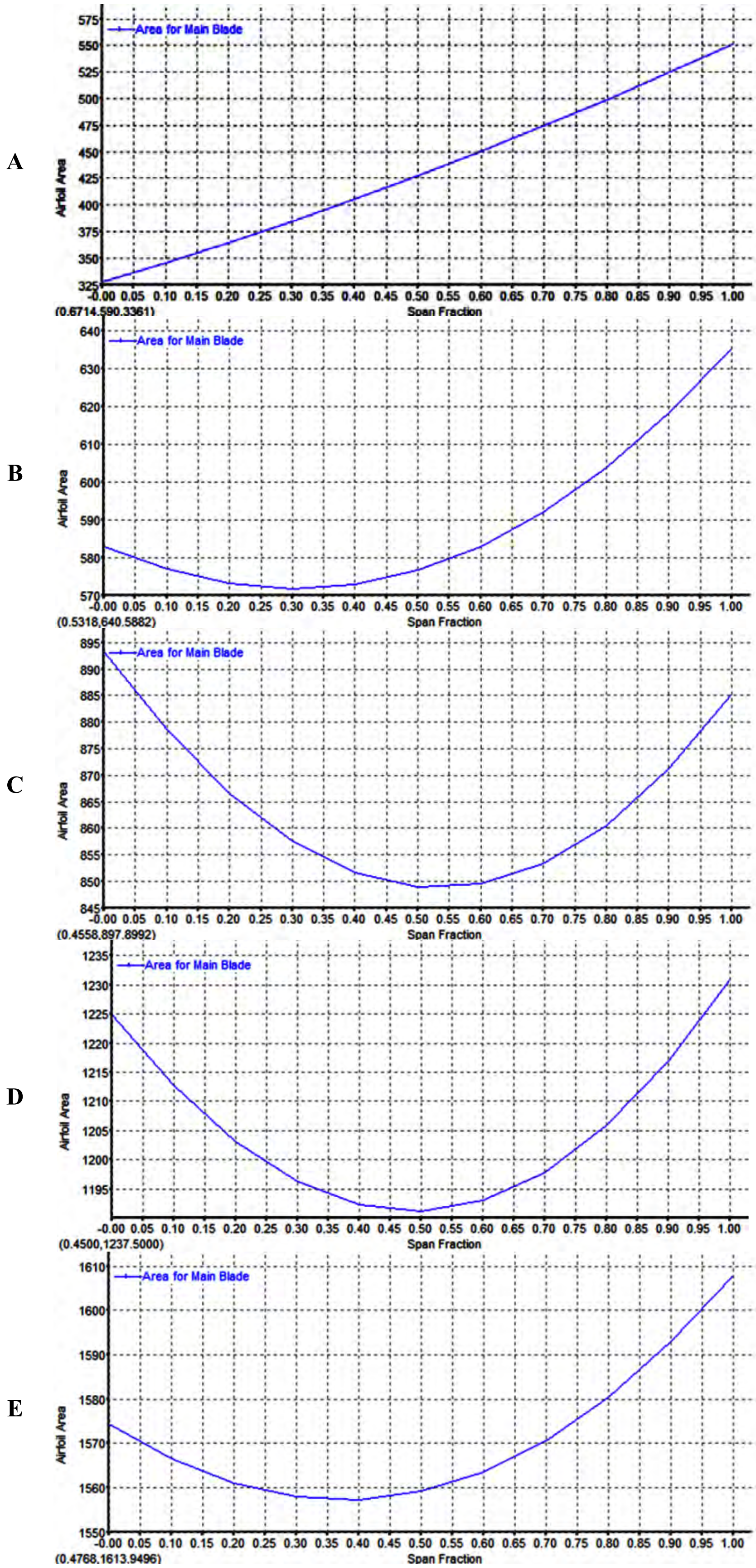

Figure 26 – The airfoil area graph: A) H = 5 m, B) H = 10 m, C) H = 15 m, D) H = 20 m, E) H = 25 m.

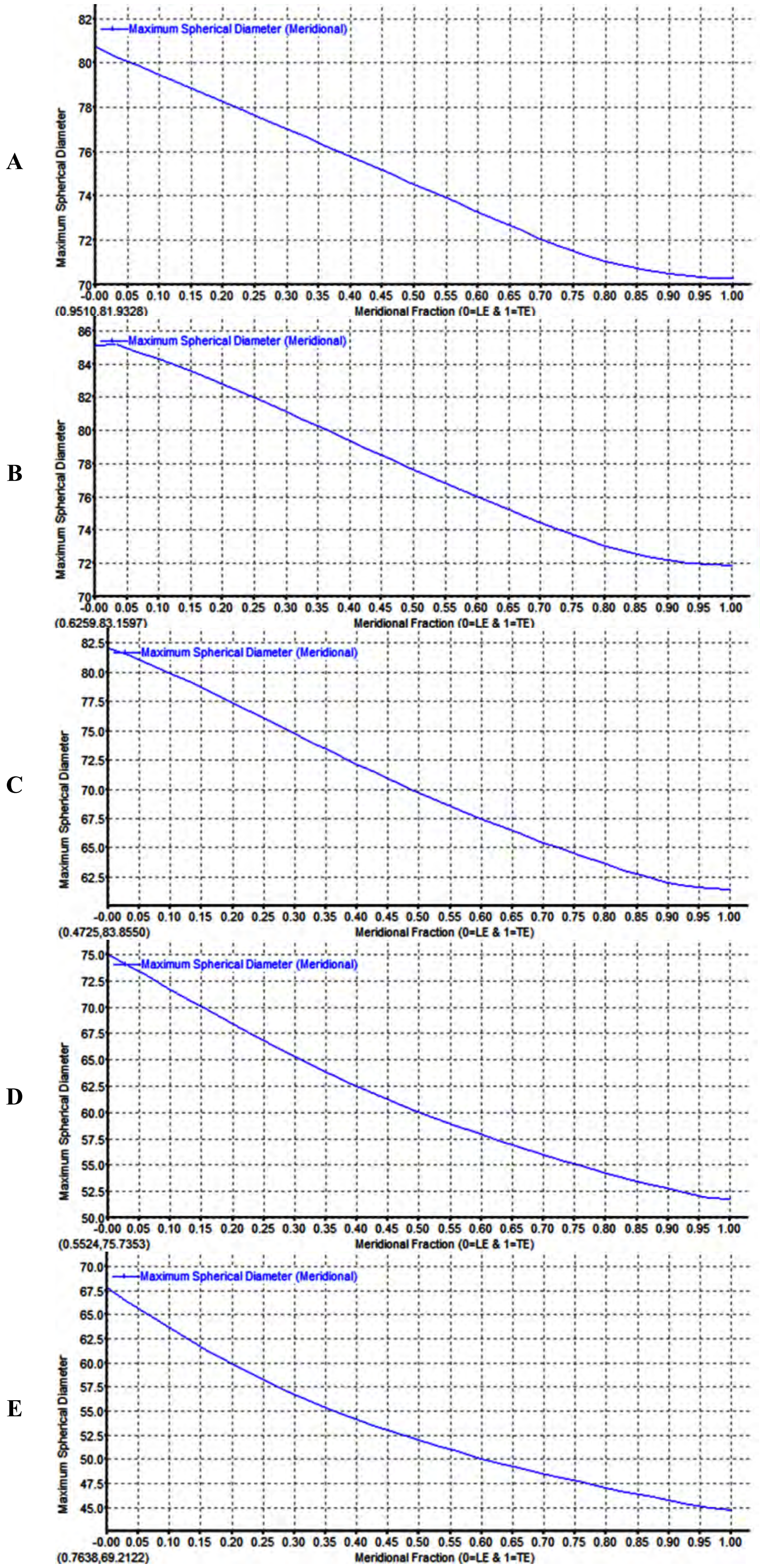

Figure 27 – The maximum diameter graph: A) *H* = 5 m, B) *H* = 10 m, C) *H* = 15 m, D) *H* = 20 m, E) *H* = 25 m.

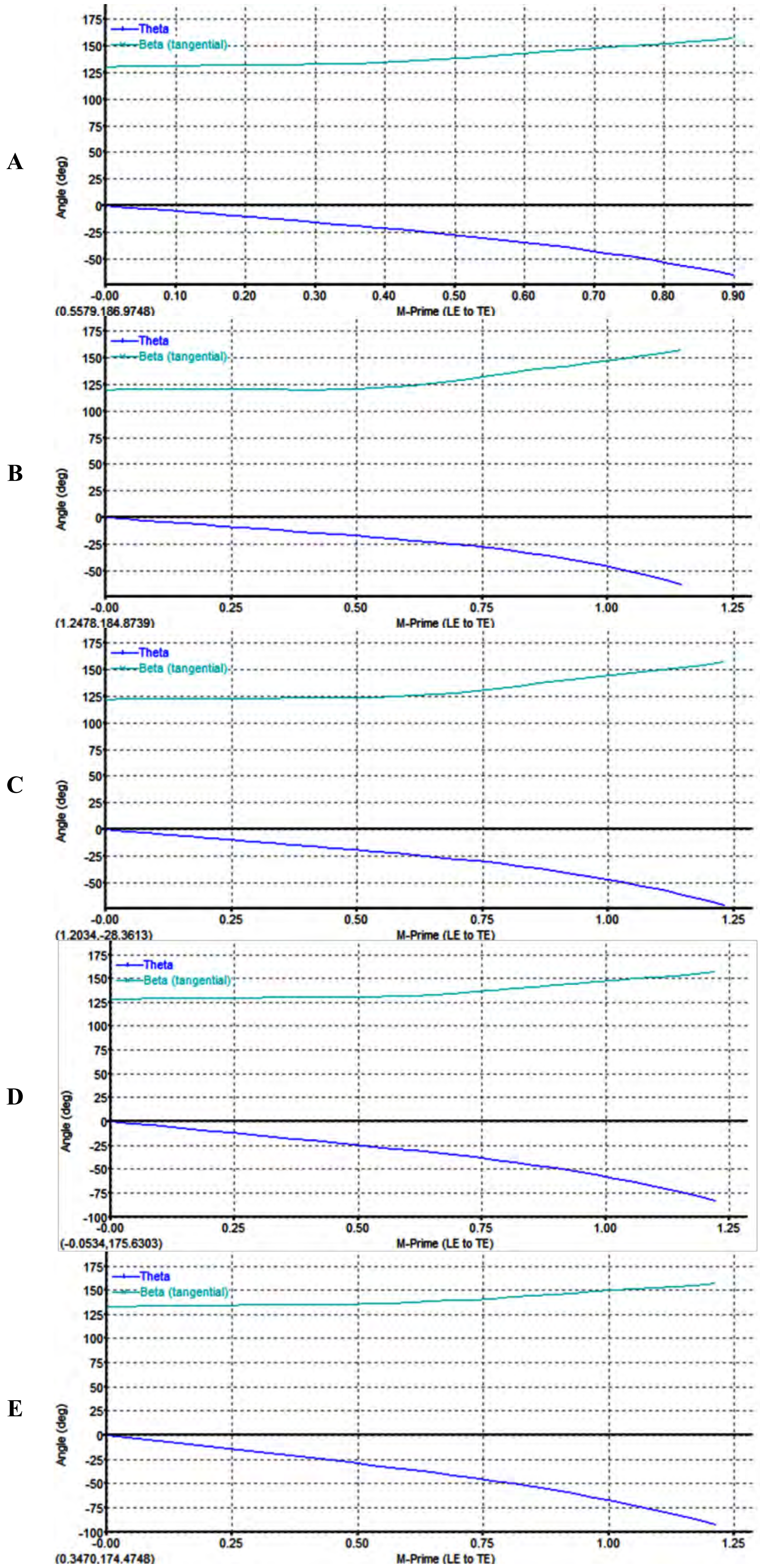

Figure 28 – The blade angle graph vs. M-prime position: A) H = 5 m, B) H = 10 m, C) H = 15 m, D) H = 20 m, E) H = 25 m.

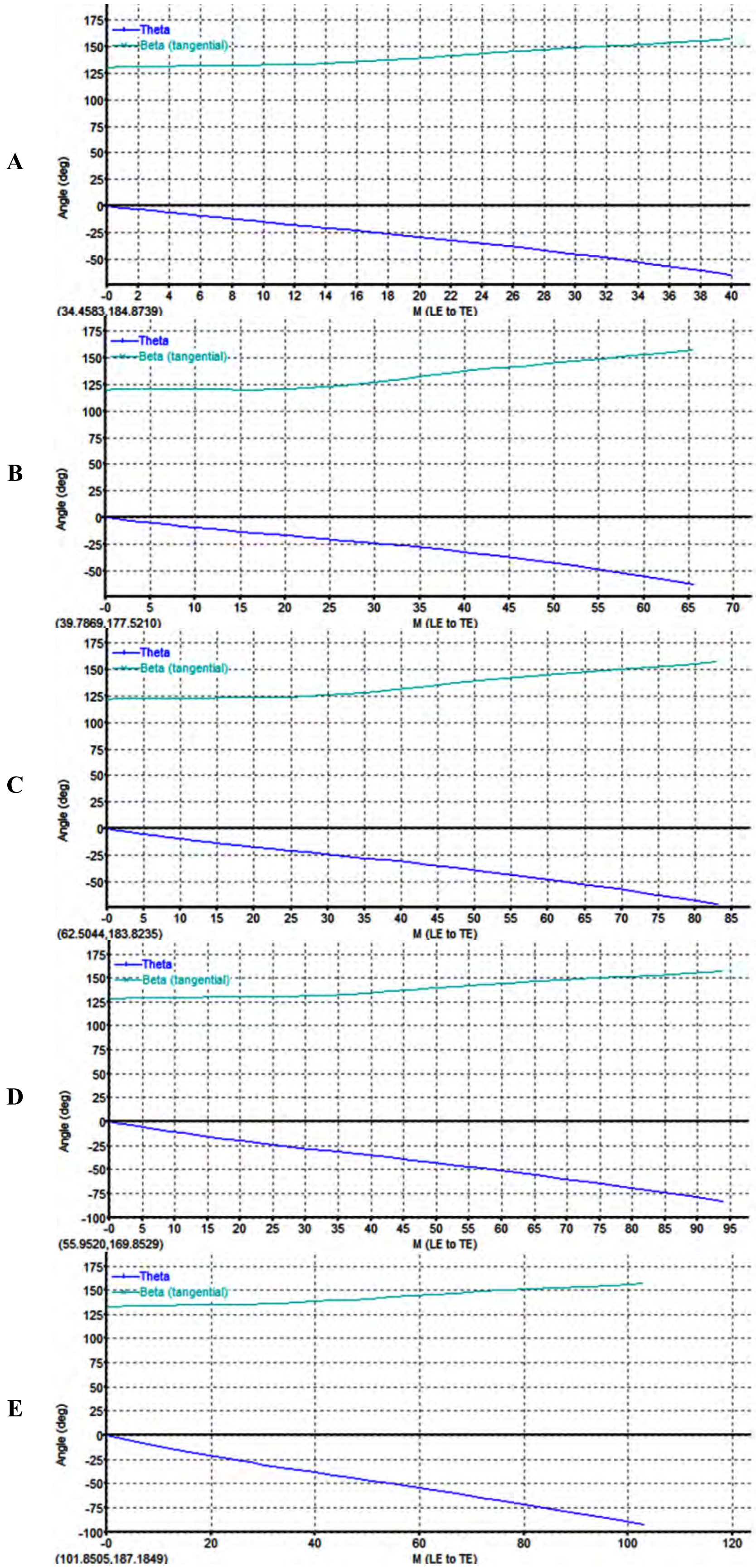

Figure 29 – The blade angle graph vs. Meridional position: A) H = 5 m, B) H = 10 m, C) H = 15 m, D) H = 20 m, E) H = 25 m.

A

B

C

D

E

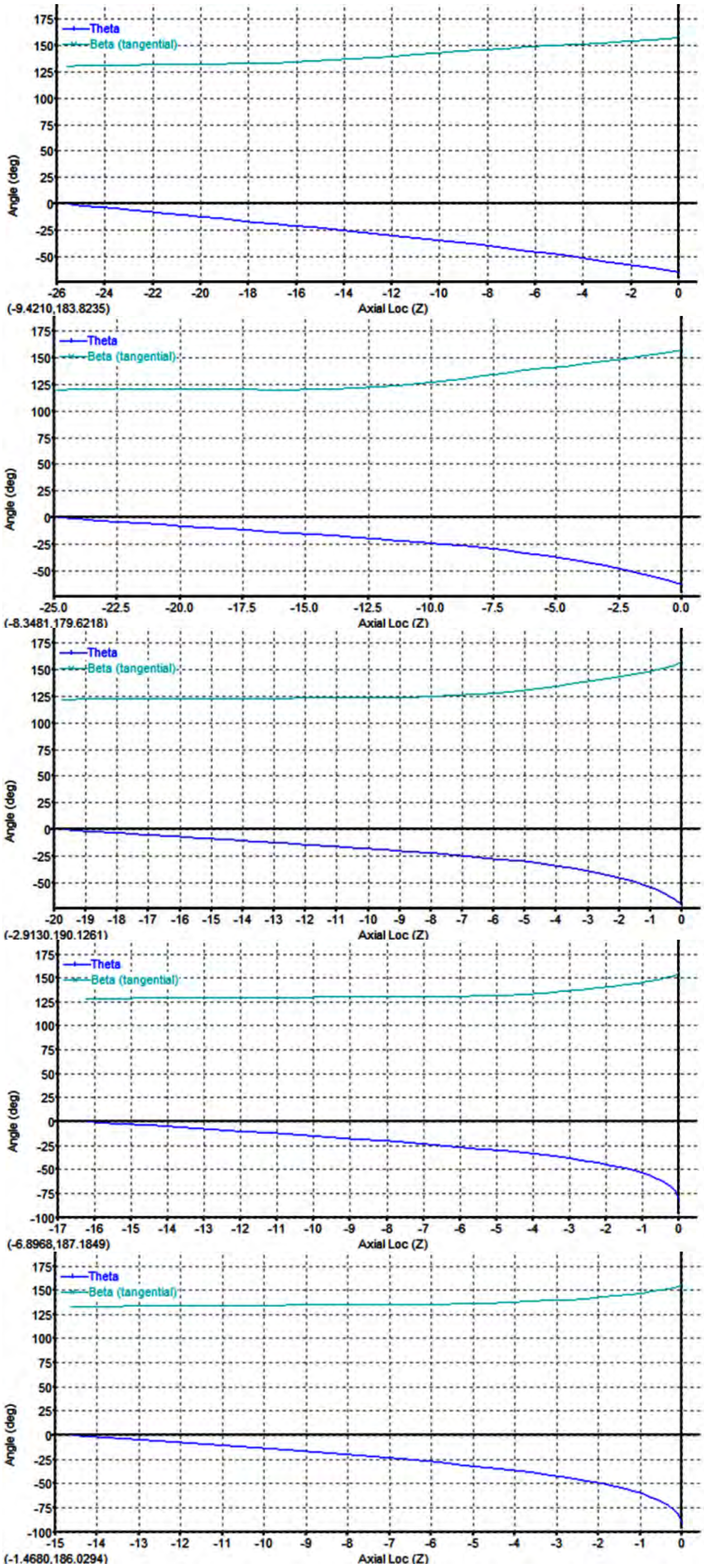

Figure 30 – The blade angle graph vs. Axial location (*Z*): A) *H* = 5 m, B) *H* = 10 m, C) *H* = 15 m, D) *H* = 20 m, E) *H* = 25 m.

A
B
C
D
E

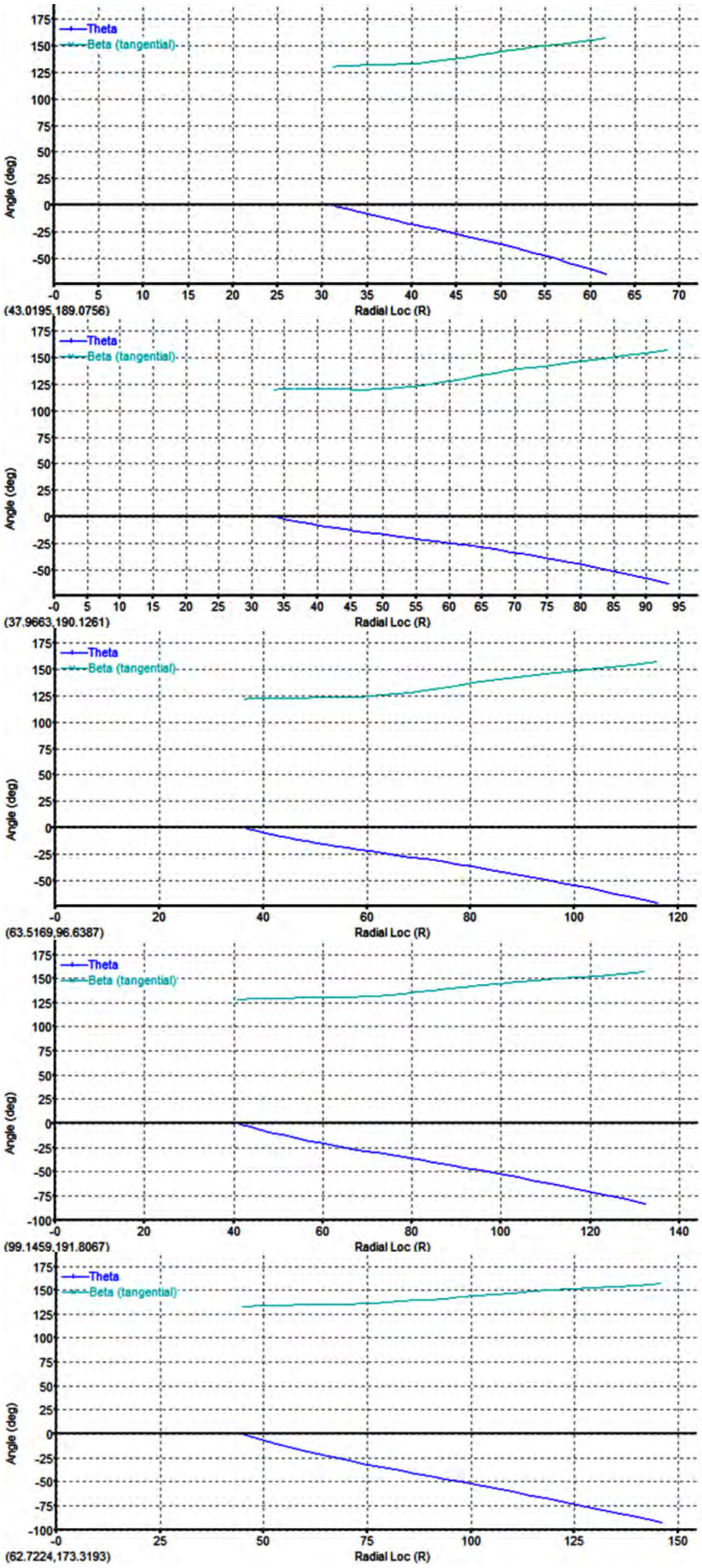

Figure 31 – The blade angle graph vs. Radial location (*R*): A) *H* = 5 m, B) *H* = 10 m, C) *H* = 15 m, D) *H* = 20 m, E) *H* = 25 m.

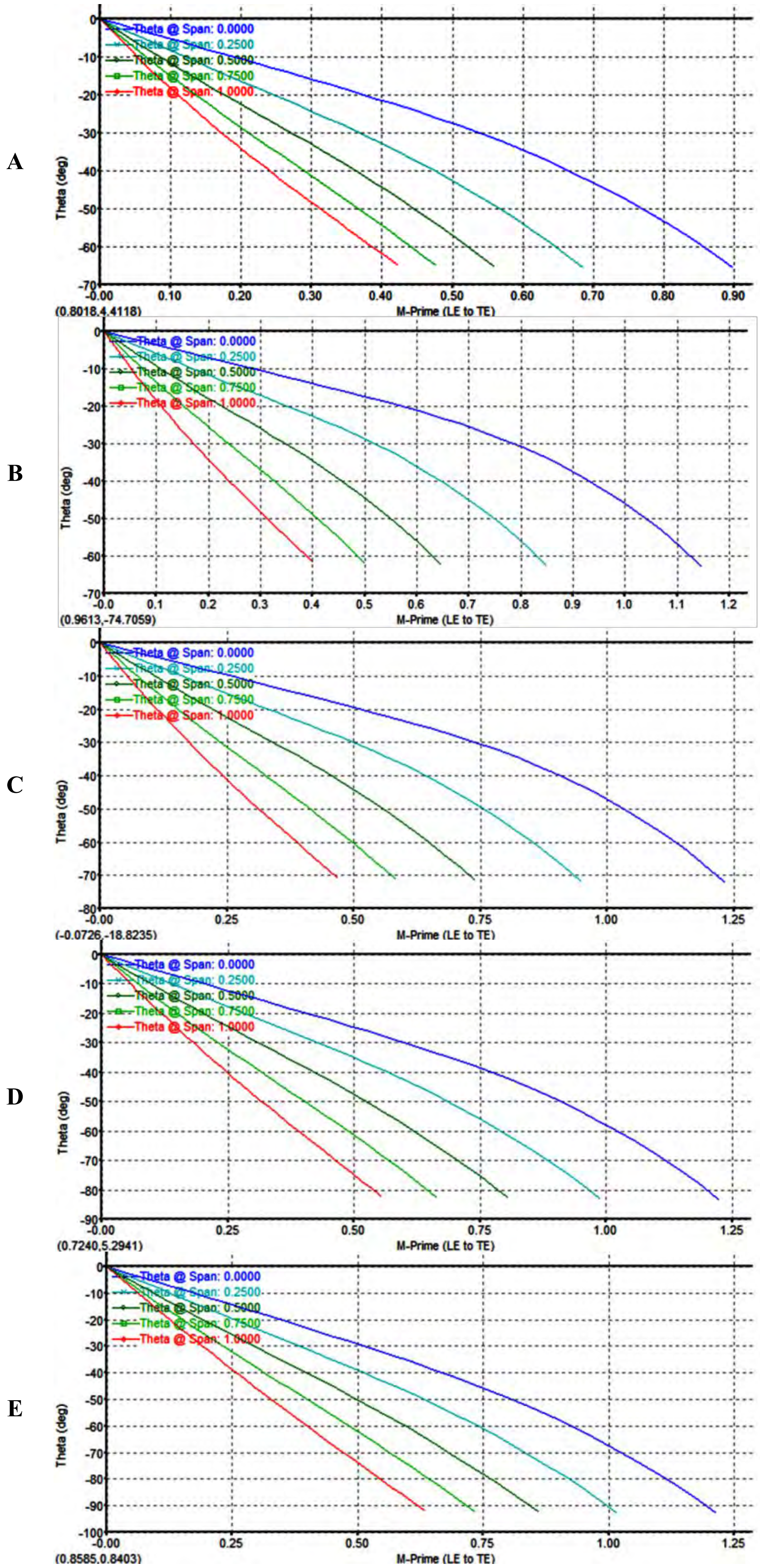

Figure 32 – The theta graph vs. M-prime position: A) H = 5 m, B) H = 10 m, C) H = 15 m, D) H = 20 m, E) H = 25 m.

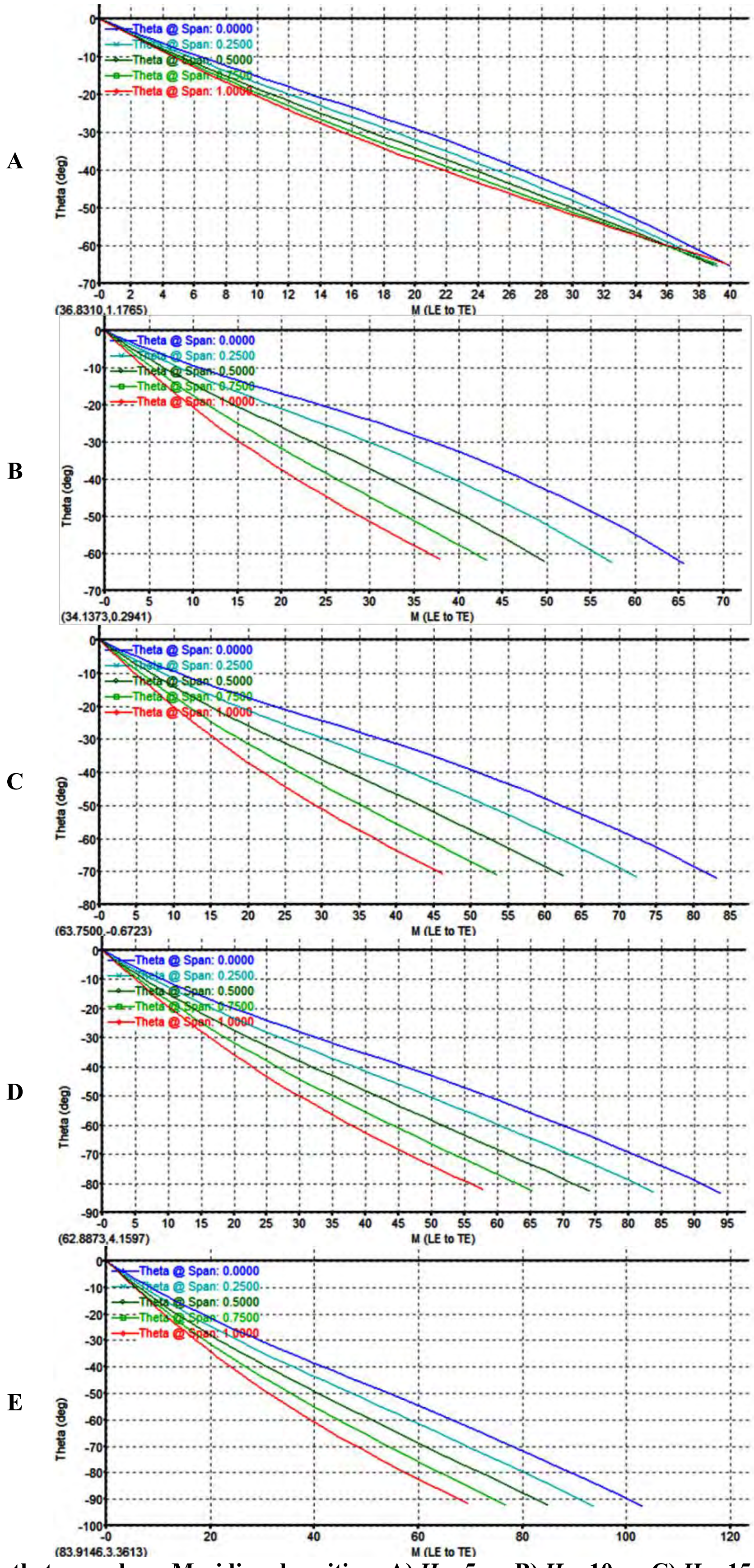

Figure 33 – The theta graph vs. Meridional position: A) *H* = 5 m, B) *H* = 10 m, C) *H* = 15 m, D) *H* = 20 m, E) *H* = 25 m.

A

B

C

D

E

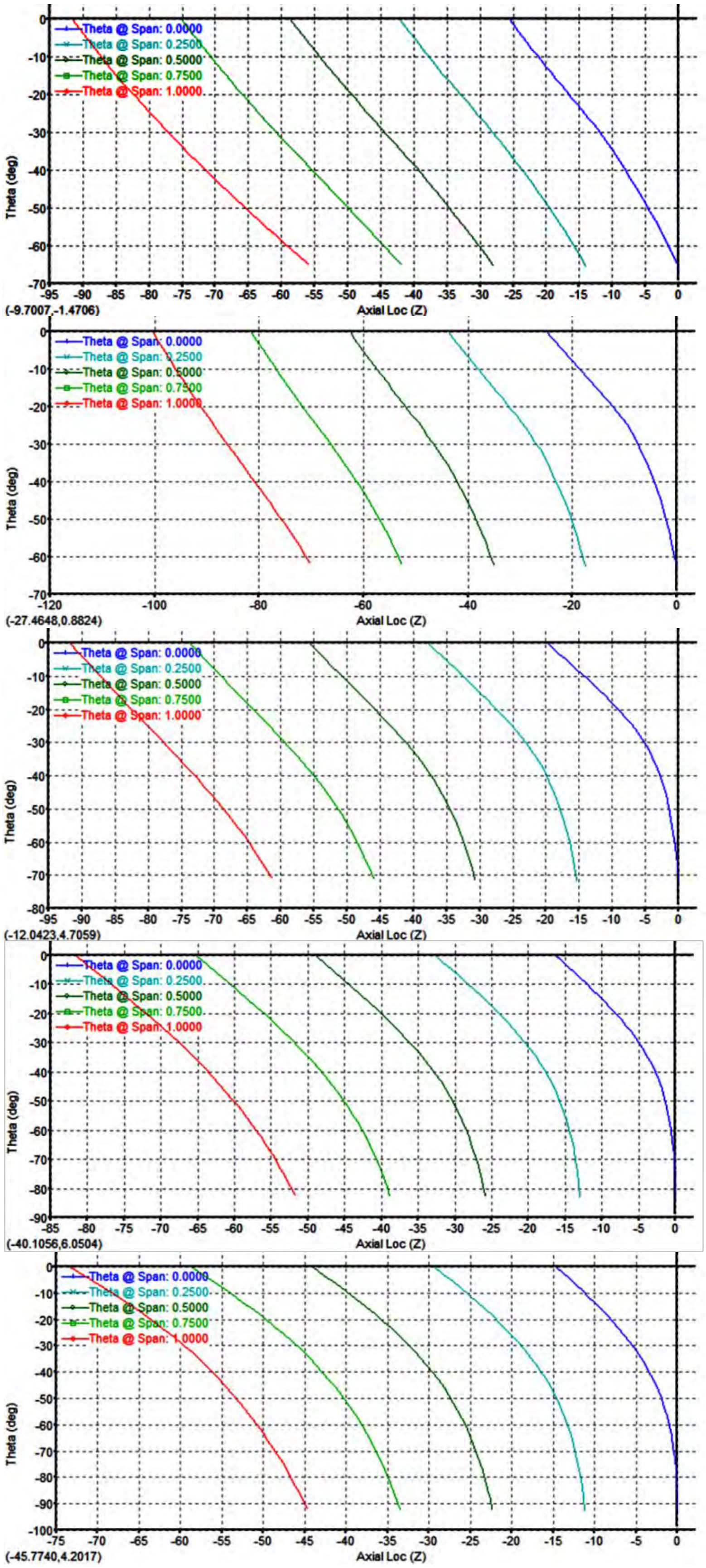

Figure 34 – The theta graph vs. Axial location (*Z*): A) *H* = 5 m, B) *H* = 10 m, C) *H* = 15 m, D) *H* = 20 m, E) *H* = 25 m.

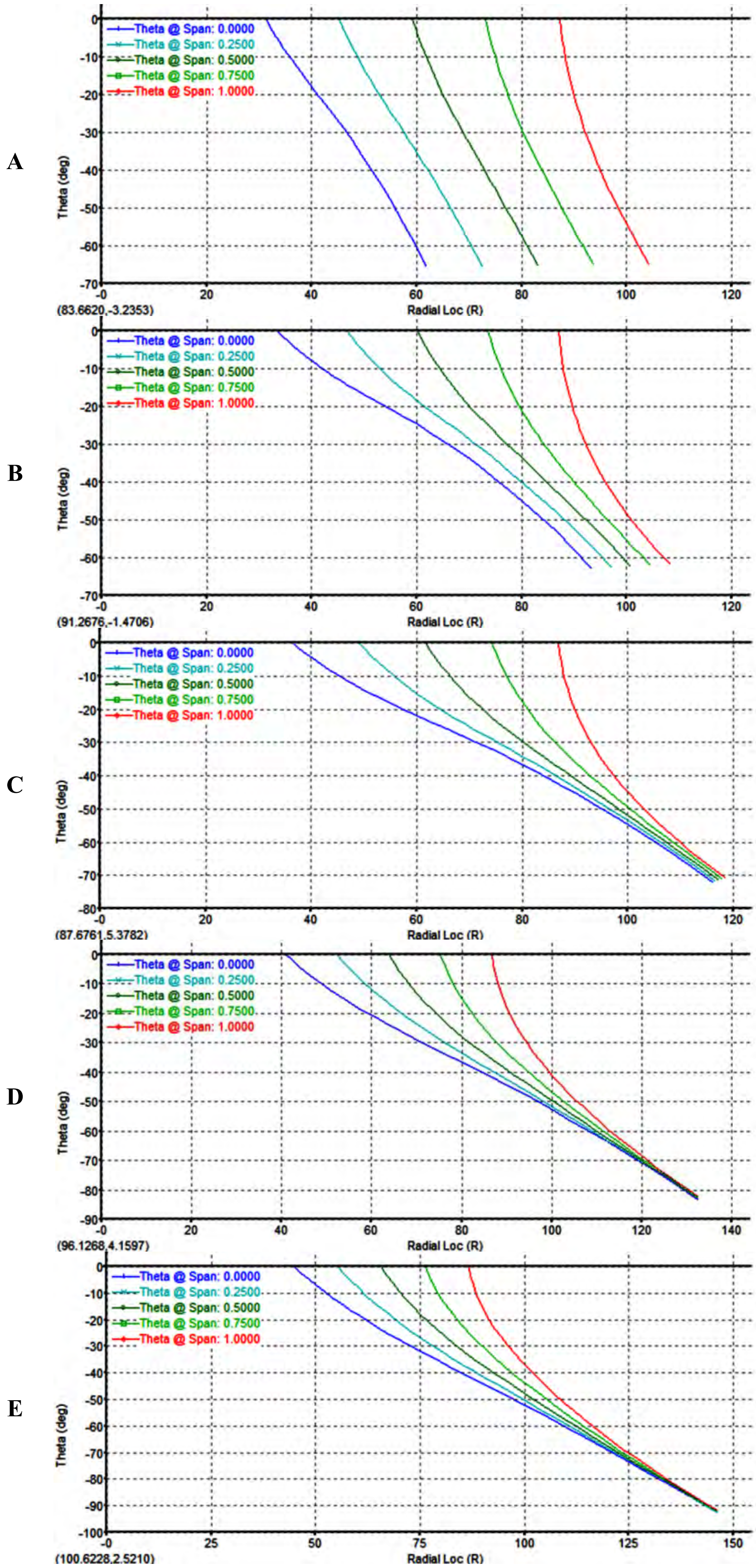

Figure 35 – The theta graph vs. Radial location (*R*): A) *H* = 5 m, B) *H* = 10 m, C) *H* = 15 m, D) *H* = 20 m, E) *H* = 25 m.

A
B
C
D
E

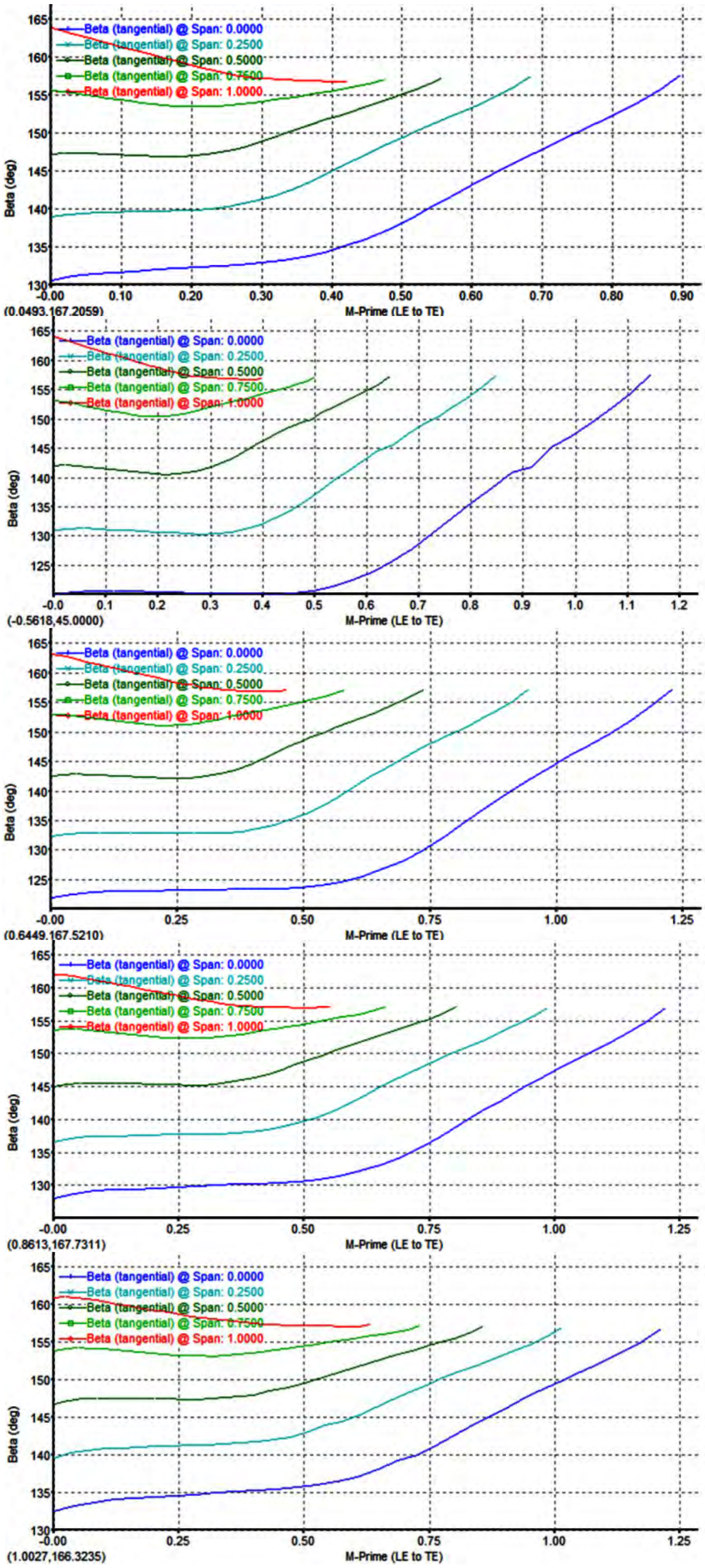

Figure 36 – The beta graph vs. M-prime position: A) *H* = 5 m, B) *H* = 10 m, C) *H* = 15 m, D) *H* = 20 m, E) *H* = 25 m.

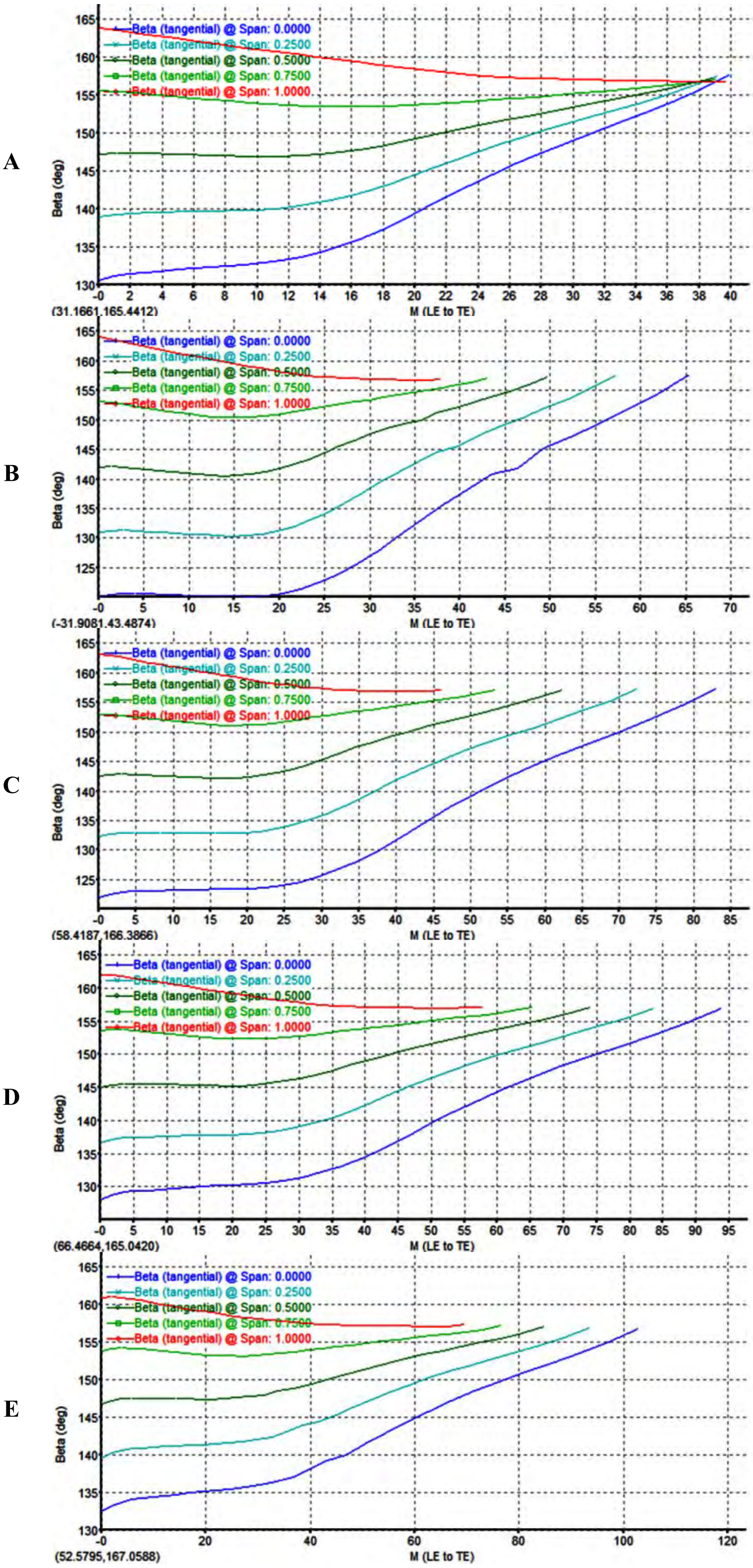

Figure 37 – The beta graph vs. Meridional position: A) H = 5 m, B) H = 10 m, C) H = 15 m, D) H = 20 m, E) H = 25 m.

A

B

C

D

E

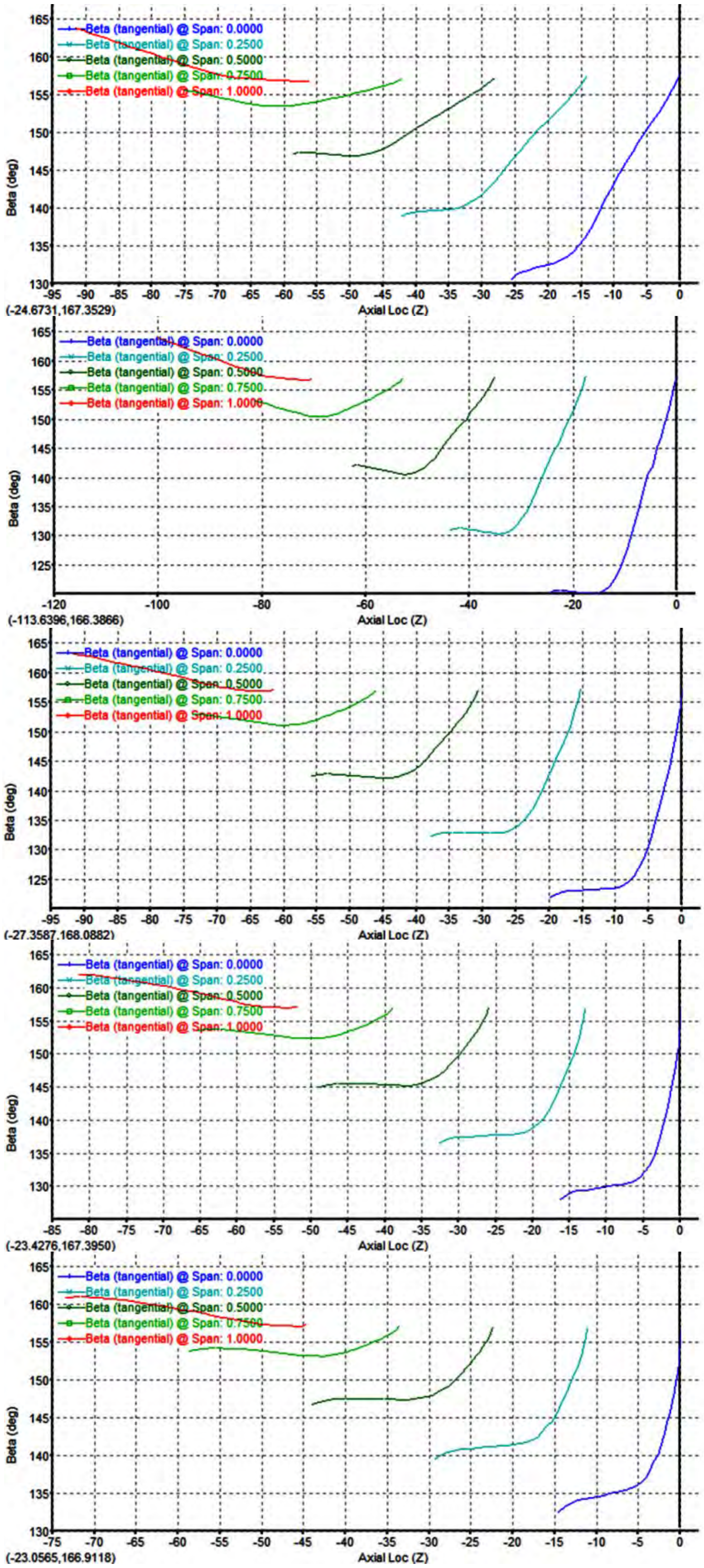

Figure 38 – The beta graph vs. Axial location (*Z*): A) *H* = 5 m, B) *H* = 10 m, C) *H* = 15 m, D) *H* = 20 m, E) *H* = 25 m.

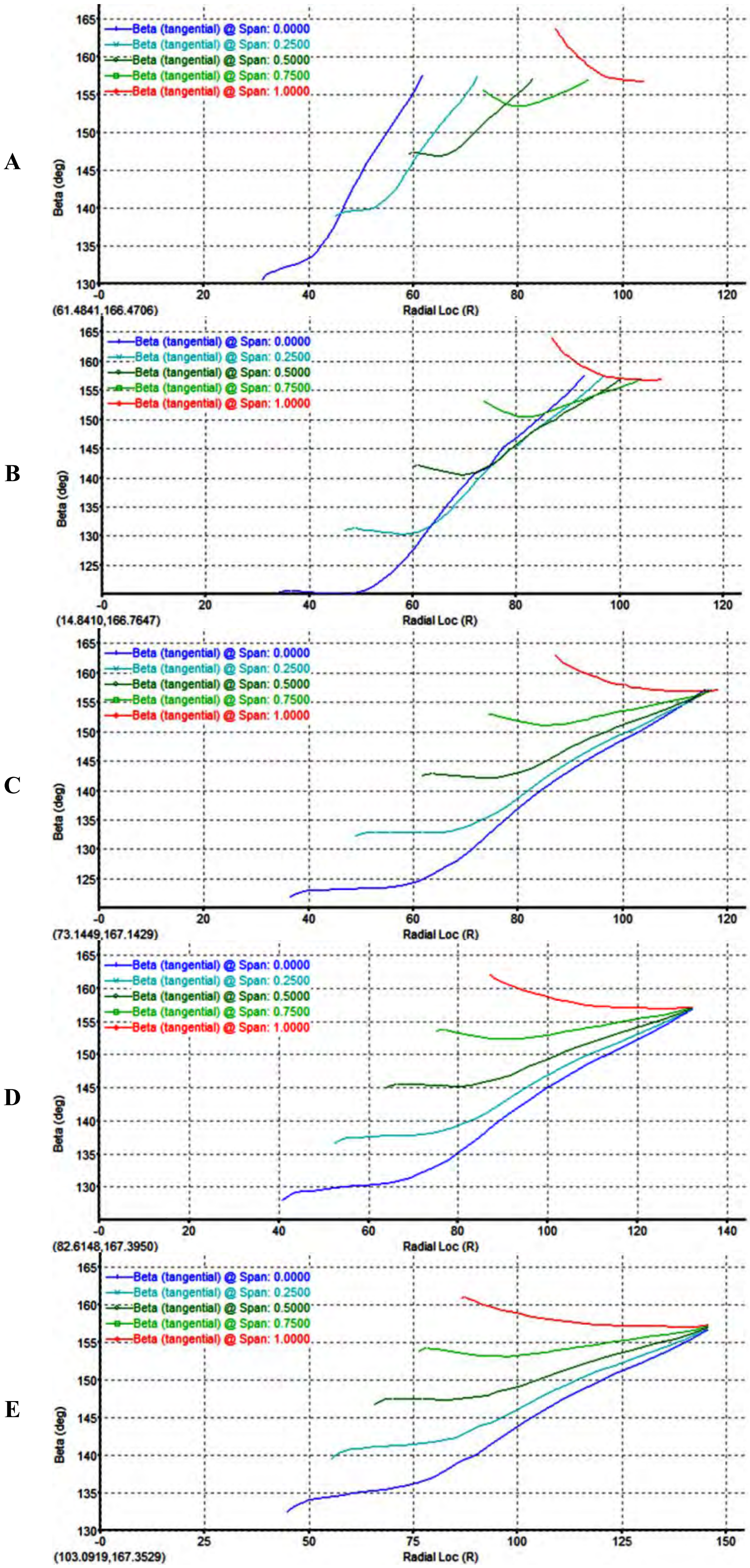

Figure 39 – The beta graph vs. Radial location (*R*): A) *H* = 5 m, B) *H* = 10 m, C) *H* = 15 m, D) *H* = 20 m, E) *H* = 25 m.

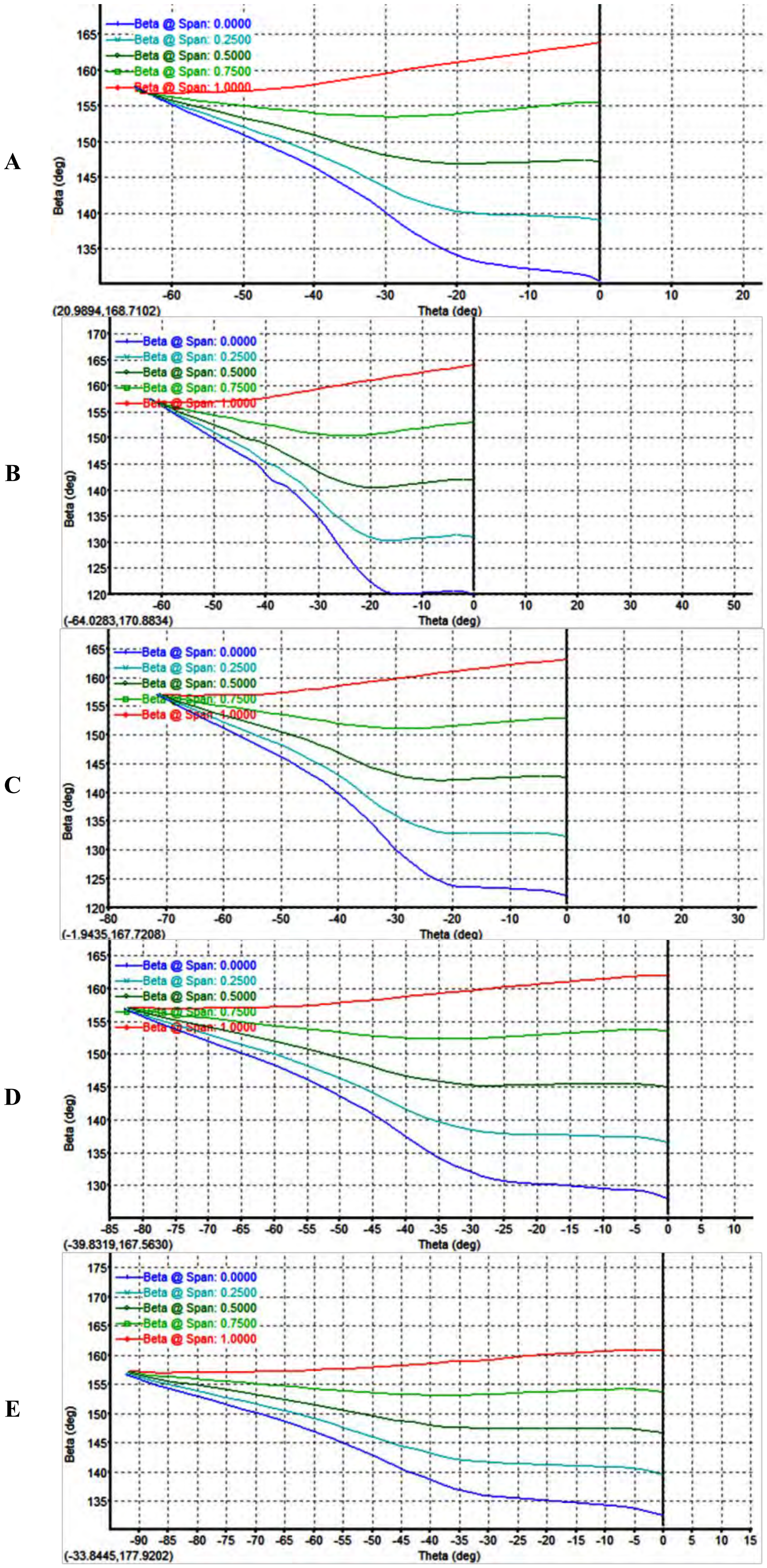

Figure 40 – The beta vs. theta graph: A) *H* = 5 m, B) *H* = 10 m, C) *H* = 15 m, D) *H* = 20 m, E) *H* = 25 m.

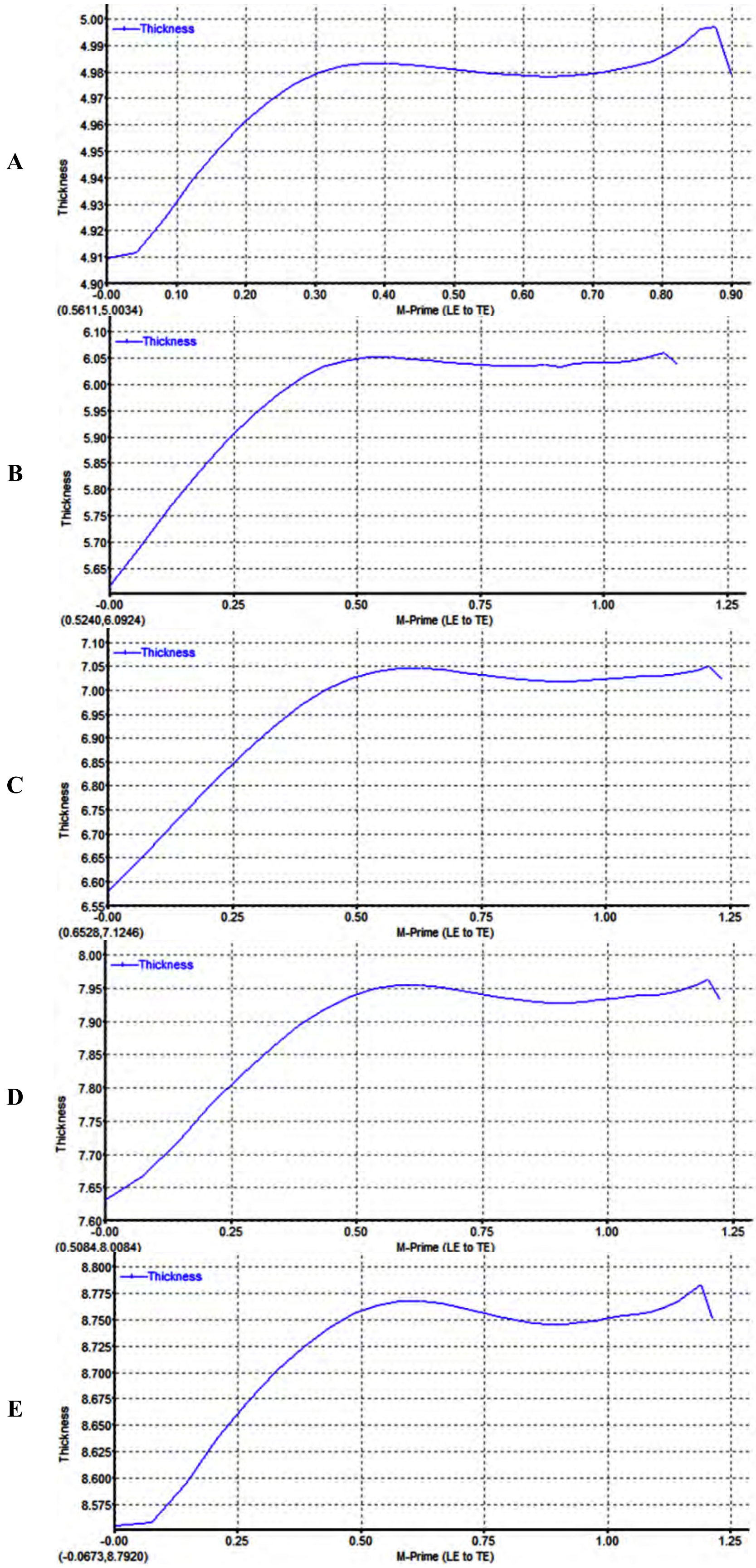

Figure 41 – The blade thickness graph vs. M-prime position: A) *H* = 5 m, B) *H* = 10 m, C) *H* = 15 m, D) *H* = 20 m, E) *H* = 25 m.

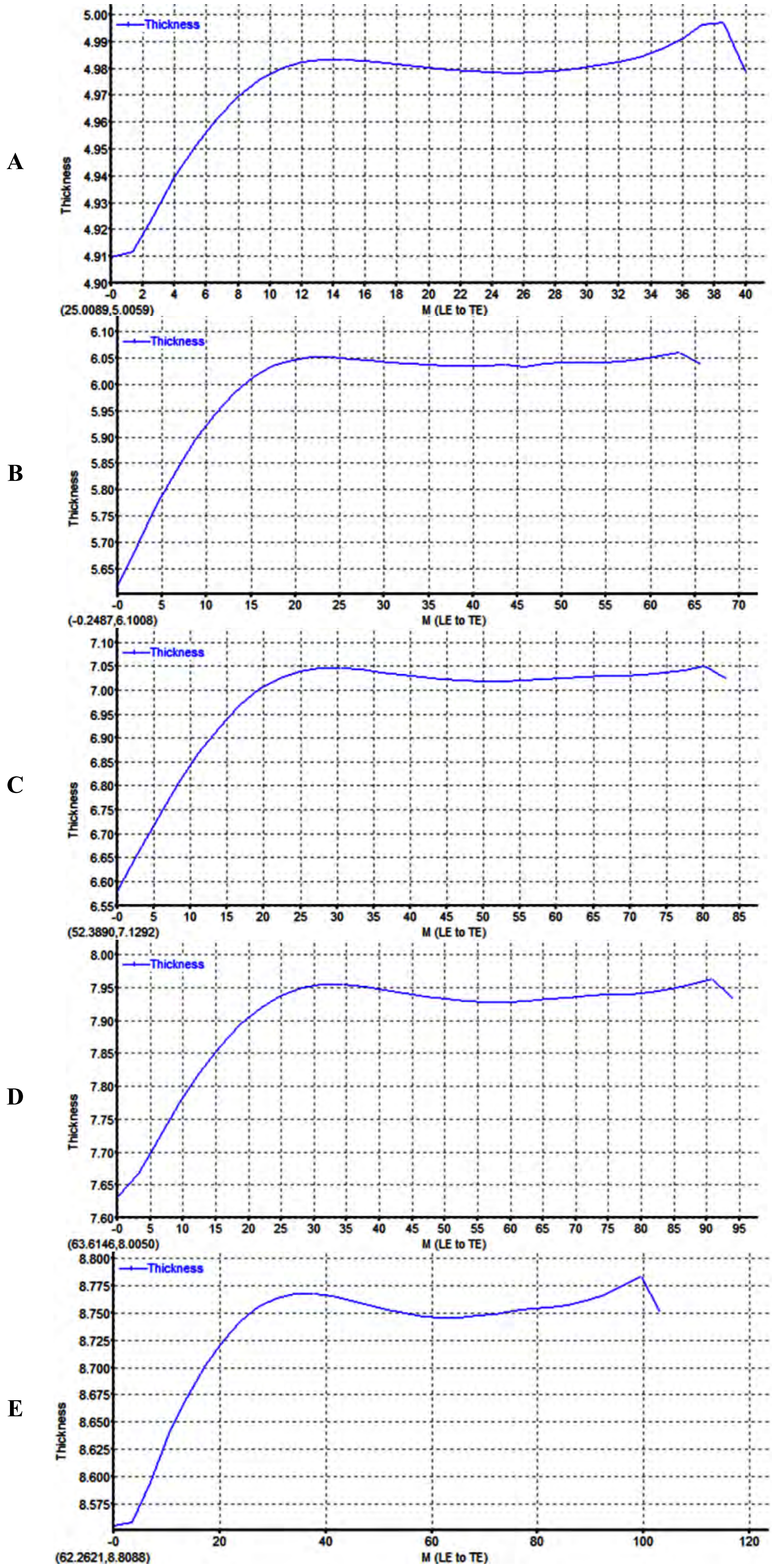

Figure 42 – The blade thickness graph vs. Meridional position: A) *H* = 5 m, B) *H* = 10 m, C) *H* = 15 m, D) *H* = 20 m, E) *H* = 25 m.

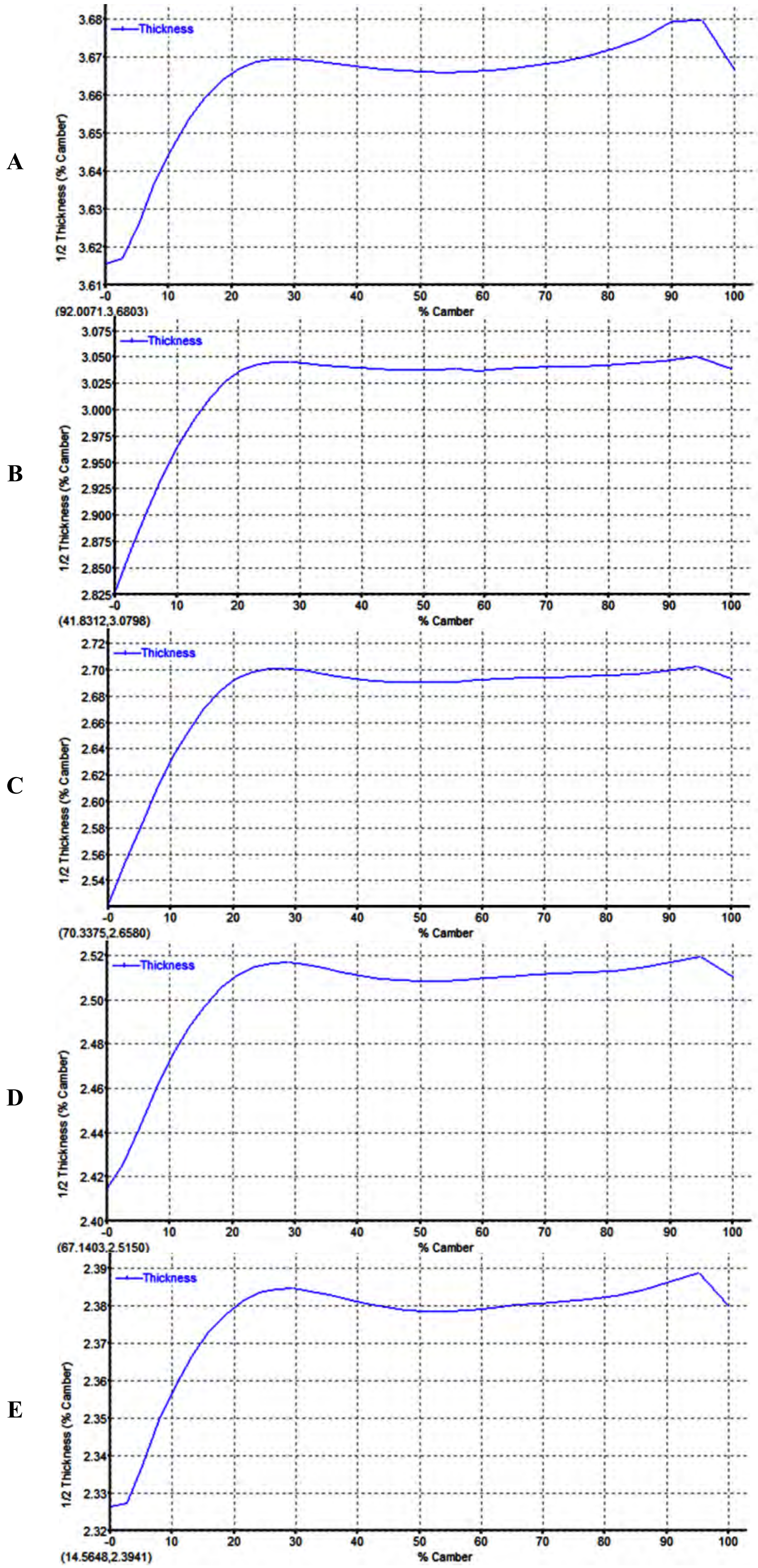

Figure 43 – The blade thickness graph – % camber vs. % camber length: A) *H* = 5 m, B) *H* = 10 m, C) *H* = 15 m, D) *H* = 20 m, E) *H* = 25 m.

A

B

C

D

E

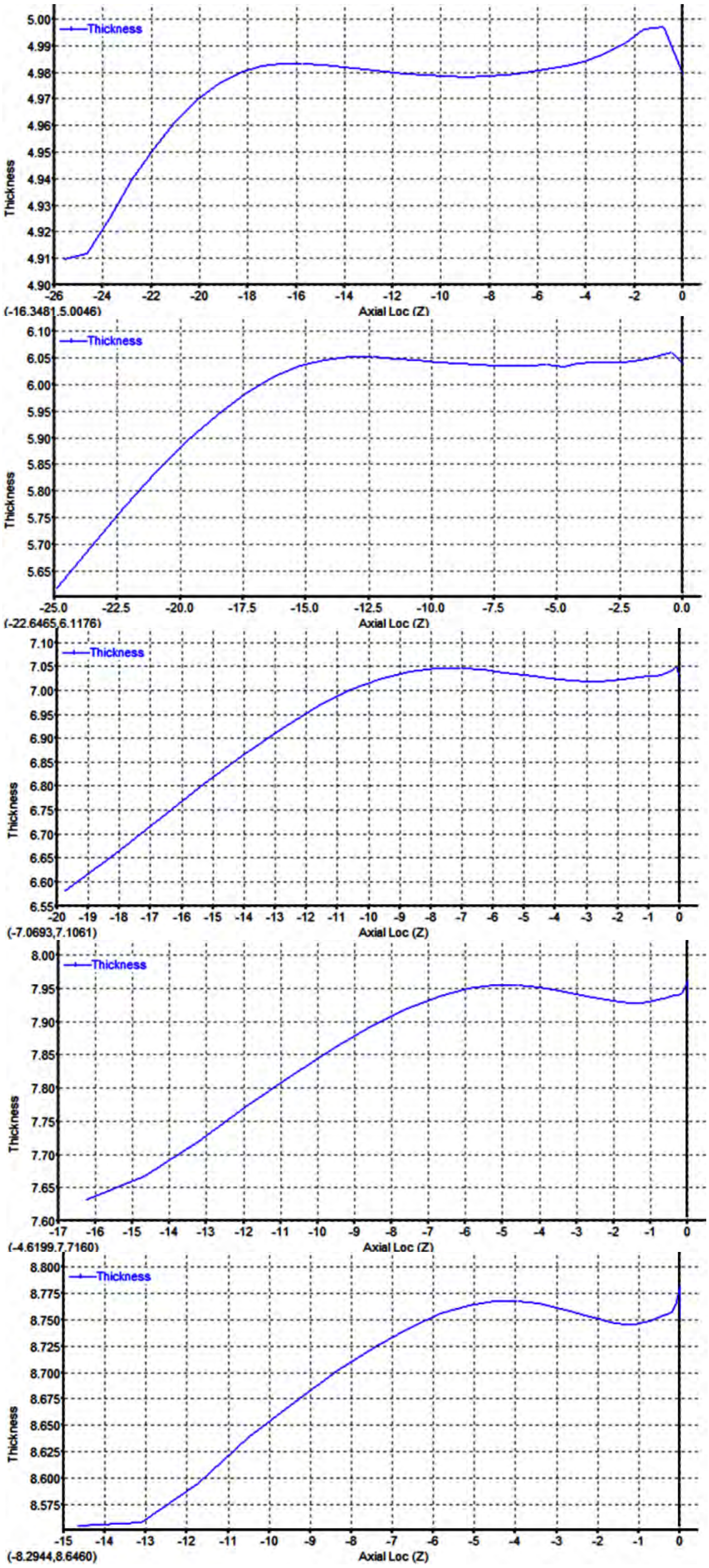

Figure 44 – The blade thickness graph vs. Axial location (*Z*): A) *H* = 5 m, B) *H* = 10 m, C) *H* = 15 m, D) *H* = 20 m, E) *H* = 25 m.

A

B

C

D

E

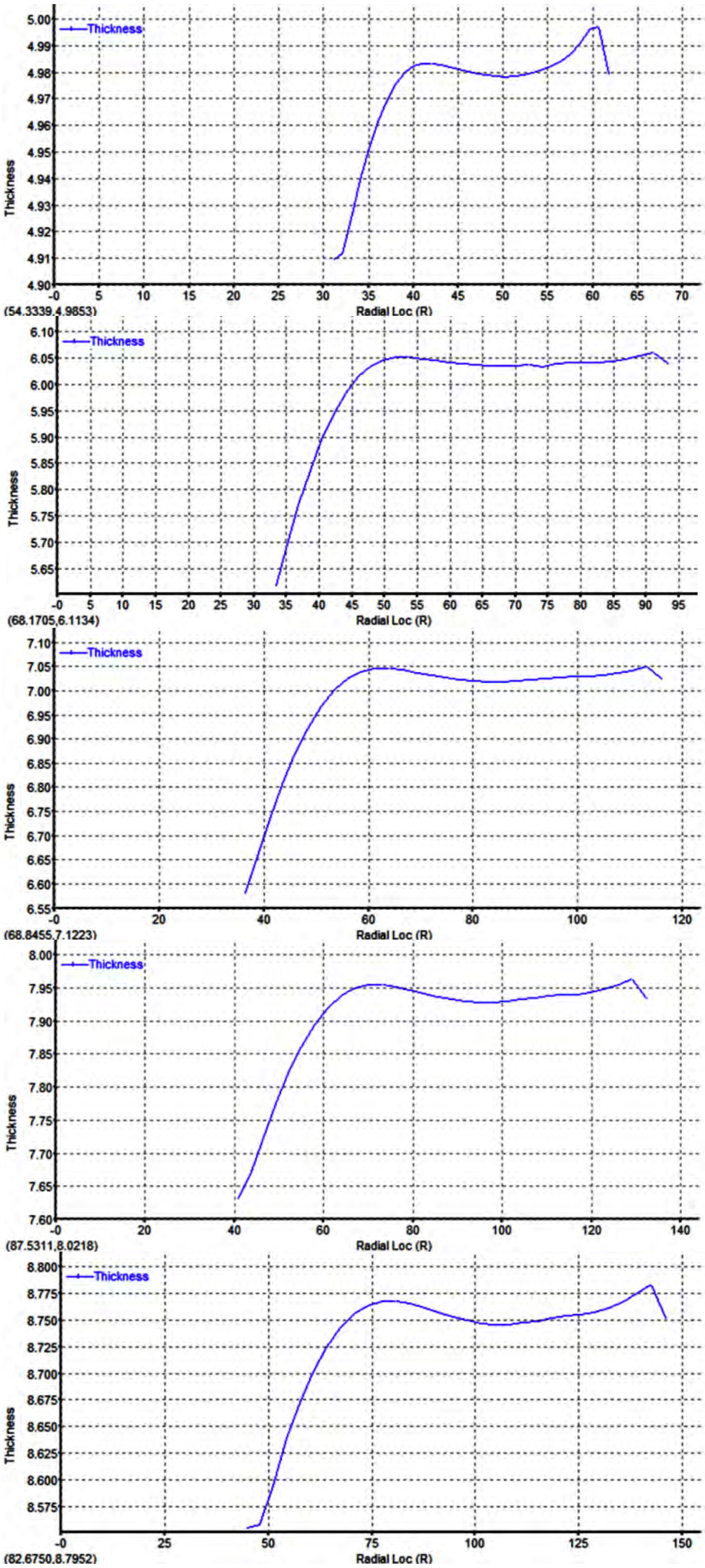

Figure 45 – The blade thickness graph vs. Radial location (*R*): A) *H* = 5 m, B) *H* = 10 m, C) *H* = 15 m, D) *H* = 20 m, E) *H* = 25 m.

The dependencies of the impellers blades thickness from *M-Prime*, *M*, *% camber length* (the current thickness graph with the vertical axis displaying the blade thickness as the percent of the total camber length and the horizontal axis displaying location as the percent of the total camber length), *Z* and *R* are calculated in the Fig. 41 – 45. These graphs are an addition to the color contours of normal thickness of the impellers blades.

The three-dimensional models of the impellers blades at the different pump heads (the Fig. 46) were built in the ***Model*** module of the ***Ansys Workbench*** software environment. The transparent volume is the created area for the calculation. The dimensions of the leading edge of the blade are presented in a foreground of the created area; the dimensions of the trailing edge of the blade are presented in a background of the created area.

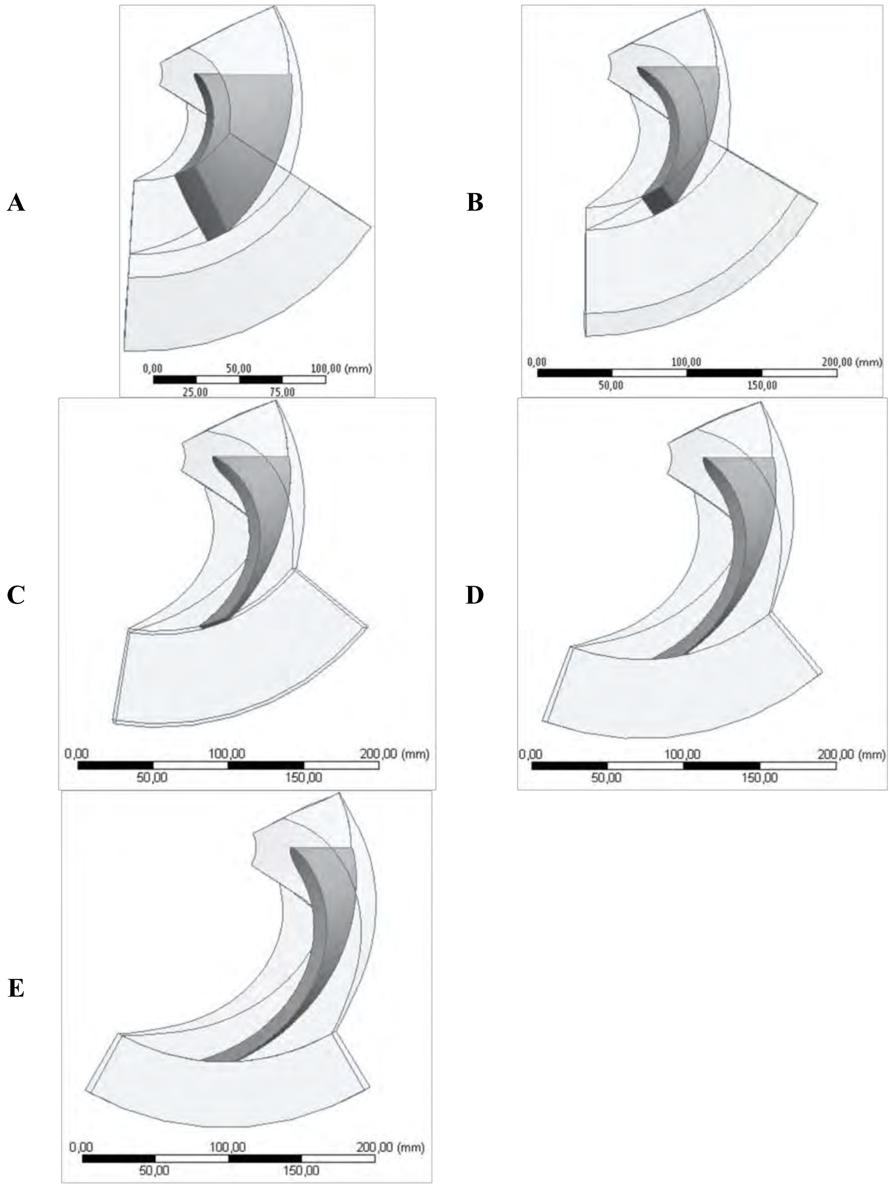

Figure 46 – The three-dimensional model of the impeller blade: A) *H* = 5 m, B) *H* = 10 m, C) *H* = 15 m, D) *H* = 20 m, E) *H* = 25 m.

Results and discussion

The calculated values of the operating and geometric parameters of the impellers at the different pump heads values are presented in the summary table 3.

The parameters of specific speed determine a geometric shape of the pump. **Ω***s* is the non-dimensional coefficient of specific speed. A type of the pump impeller is determined by the value of this coefficient. It is necessary to choose the mixed flow impeller at the pump head is 5 – 15 m. The radial impeller is selected at the pump head more than 20 m. *Ns* and *nq* are equivalent forms of **Ω***s*. These parameters are used for the calculation of specific speed of the pump in Europe and the USA.

Table 3. The calculated operating and geometrical parameters of the impellers/pump.

Overall performance

Pump head, m	*Ωs*	*Ns*	*nq*	*Nss*	*Power, kW*	*Head coeff*	*Flow coeff*	*Ks*	*NPSHr, m*	*Diffn ratio*
5	2.48	6789	131.5	3.15	5.6	0.289	0.239	0.87	3.64	0.088
10	1.48	4037	78.2	3.15	10.5	0.392	0.134	0.897	3.64	0.121
15	1.09	2978	57.7	3.15	15.7	0.435	0.085	0.953	3.64	0.101
20	0.88	2400	46.5	3.15	20.9	0.455	0.059	0.996	3.64	0.073
25	0.74	2030	39.3	3.15	26.2	0.467	0.044	1.028	3.64	0.049

Impeller inlet

Pump head, m	*D1, mm*	*Cu1, m/s*	*Cm1, m/s*	*U1, m/s*	*W1, m/s*	*β'1, deg*	*β1, deg*	*Inc, deg*	*Dh, mm*	*De, mm*	*Thk, mm*
5	62.3	0	3.69	4.9	6.13	42.65	37.01	5.65	25.6	172.6	5
	118.4	0	4.1	9.3	10.16	25.88	23.8	2.08			
	174.4	0	4.51	13.7	14.42	18.23	18.23	0			
10	66.7	0	3.84	5.24	6.5	41.84	36.23	5.61	31.6	172.6	6
	120.3	0	4.27	9.45	10.37	26.41	24.3	2.11			
	173.9	0	4.69	13.66	14.44	18.97	18.97	0			
15	72.9	0	4.14	5.73	7.07	41.49	35.89	5.6	36.1	172.6	7
	123.3	0	4.6	9.68	10.72	27.61	25.43	2.18			
	173.7	0	5.06	13.64	14.55	20.37	20.37	0			
20	81.7	0	4.51	6.42	7.85	40.65	35.09	5.56	39.7	172.6	7.9
	127.6	0	5.01	10.02	11.21	28.81	26.56	2.25			
	173.5	0	5.51	13.63	14.7	22.02	22.02	0			
25	89.7	0	4.89	7.05	8.58	40.32	34.77	5.55	42.8	172.6	8.8
	131.6	0	5.44	10.33	11.68	30.05	27.74	2.31			
	173.4	0	5.98	13.62	14.88	23.7	23.7	0			

Impeller exit

Pump head, m	*D2, mm*	*B2, mm*	*Lean, deg*	*β2, deg*	*W2, m/s*	*α2, deg*	*C2, m/s*	*Wslip/U2*	*U2, m/s*	*Cu2, m/s*
5	166	71.5	0	19.37	9.26	35.53	5.28	0.1	13.04	4.3
10	201.3	68.6	0	16.84	9.11	20.42	7.57	0.15	15.81	7.09
15	234.2	57.3	0	16.35	9.64	16.53	9.54	0.15	18.4	9.14
20	264.5	47.8	0	16.12	10.39	14.95	11.17	0.15	20.78	10.8
25	291.7	40.9	0	15.96	11.11	14.01	12.61	0.14	22.91	12.24

Suction specific speed *Nss* characterizes intensity of the pump cavitation. The calculated values of *Nss* were 3.15. This indicates about good cavitation characteristic of the pump. The shaft power is increased in average by 5.2 kW at increasing of the pump head by 5 m. The head coefficient ψ has characteristic of energy transfer measure to fluid. Maximum difference of energy transfer to fluid was determined at the small values of the pump head. Changing determination of flow rate through the pump is carried out by the value of the flow coefficient. The flow coefficient is 0.239 at the pump head of 5 m, the flow coefficient is 0.044 at the pump head of 25 m. The stability factor *Ks* determines stable characteristic of the pump performance. Unstable characteristic of the pump performance is observed at head of 5 and 10 m ($Ks < 0.9$). Net positive suction head required (*NPSHr*) for the pump performance provides reduction of noise and damage due to cavitation. *NPSHr* for all considered pumps is 3.64 m. The diffusion ratio determines stable of head-flow curve. Maximum stable was determined at the diffusion ratio is 0.049; minimum stable was determined at the diffusion ratio is 0.121.

The hub diameter (*Dh*) changes by 17.2 mm at increasing of the pump head by 20 m and the eye diameter (*De*) does not change (172.6 mm). The blades thickness of the impellers is increased in the range from 5 to 8.8 mm with increasing of the pump head. The values of the diameter (*D1*), tangential velocity (*Cu1*), meridional velocity (*Cm1*), the blade speed (*U1*), flow relative velocity (*W1*), the blade angle ($\beta'1$), relative flow angle ($\beta 1$) and incidence (*Inc*) were calculated in the sections of the hub, the mean line and the shroud of the impellers. Incidence is calculated as difference of the angles of $\beta'1$ and $\beta 1$. Increasing of the *D1* parameter at the hub and decreasing at the shroud is required with increasing of the pump head. Tangential velocity was not taken into account. Maximum meridional velocity is achieved at the impeller shroud. The blade speed of the impeller increases in the sections of the hub and the mean line. Flow relative velocity of fluid at the impeller inlet varies from 6.13 to 14.88 m/s. Maximum changing of flow relative velocity of fluid is determined at the impeller hub. The blade angle of the impeller decreases at the hub, the relative flow angle increases at the mean line. The values of $\beta'1$ and $\beta1$ are equal at the shroud.

The calculated parameters at the impeller trailing edge were written in the title ***Impeller exit*** (the table 3). The tip diameter (*D2*) changes in average by 31 mm at changing of the pump head by 5 m. Maximum changing of the tip width of the impeller (*B2*) is observed at the pump head of 10 – 20 m. The calculated value of the lean angle was 0 degrees according to the results of five researches. The ratios of *U1* to tip speed at the impeller outlet (*U2*) are from 0.375 to 0.594. Flow relative velocity at the impeller outlet (*W2*) is higher than *W1* at the hub and lower than at the mean line and the shroud. Relative flow angle ($\beta2$) at the impeller outlet is less than at the inlet. The absolute flow angle ($\alpha2$) is more than $\beta2$ at the pump head values of 5 – 15 m. Flow tangential velocity (*Cu2*) at the impeller outlet increases in the range of 4.3 – 12.24 m/s, i.e. increases in 3 times at increasing of the pump head in 5 times. The values of flow absolute velocity (*C2*) at the impeller outlet were determined in the range of 5.28 – 12.61 m/s. The slip factor (*Wslip/U2*) characterizes the deviation degree of fluid flow from the impeller blade. The minimum degree of deviation of fluid flow is calculated at the pump head of 5 m and the corresponding geometry of the impeller blade.

Conclusion

Based on the performed analysis of the designed geometry of the impellers in conditions of changing of the pump head, it is possible to draw the following conclusions:

1. The impeller blades with the larger profile curvature should be made at the pump head of more than 20 m.
2. Required performance of the pump (by conditions of the performed experiments) is provided by the mixed flow impellers at the pump head of up to 15 m and the radial impellers at the pump head of more than 20 m.
3. The surfaces cavitation of the impellers occurs with the same intensity at the different pump heads and geometric characteristics of the blades.
4. Stable characteristic of the pump is observed at operation of the radial impellers with the calculated geometry. The calculated geometry of the impeller at the pump head of less than 10 m leads to unstable characteristic of the pump.
5. Calculated deviation of fluid flow from the impeller blade at the pump heads of 10 – 20 m is more by 5% than at the pump head of 5 m.

References:

1. Baljé, O. (1981). *Turbomachines - a guide to design, selection and theory.* J. Wiley & Sons, New York.
2. Smith, A. G. (1957). On the generation of the Streamwise Component of Vorticity for Flows in a Rotating Passage. *Aeronautical Quartely, Vol. 8*, 369-383.
3. Rusetskaya, G. V. (2005). Mathematical model of a liquid - discharge channel system of a radial impeller pump. *Chemical and petroleum engineering, vol. 41, issue 7-8*, 377-382.
4. Ben-Nun, R., Sheintuch, M., Kysela, B., Konfršt, J., & Fořt, I. (2015). Semianalytical characterization of turbulence from radial impellers, with experimental and numerical validation. *Aiche Journal, issue 4, vol. 61*, 1413-1426.
5. Van den Braembussche, R. A. (2006). *Optimization of Radial Impeller Geometry. In Design and Analysis of High Speed Pumps* (pp. 13-1 – 13-28). Educational Notes RTO-EN-AVT-143, Paper 13. Neuilly-sur-Seine, France: RTO.
6. Harinck, J., Alsalihi, Z., Van Buijtenen, J. P., & Van den Braembussche, R. A. (2005). *Optimization of a 3D Radial Turbine by means of an improved Genetic Algorithm.* Proceedings of the 5th European Conference on Turbomachinery. (pp.1033-1042).
7. Lewis, R. I. (1996). *Turbomachinery Performance Analysis.* Elsevier Science & Technology Books.
8. Chemezov, D. A. (2016). The parameters of the gas turbine blade when changing of the ratio of the output/input radius of the hub. *ISJ Theoretical & Applied Science, 02 (34)*, 75-85.
9. Epple, P., Miclea, M., Luschmann, C., Llic, C., & Delgado, A. (2010). *An extended analytical and numerical design method with applications of radial fans.* Proceedings ASME International Mechanical Engineering Congress and Exposition. (pp.1119-1129).
10. Chemezov, D. A. (2015). Computer design and analysis of pressure distribution on the surface of the blade of the impeller radial turbine. *ISJ Theoretical & Applied Science, 01 (21)*, 1-6.